

# Effects of Synthetic Air Entraining Agents on Compressive Strength of Portland Cement Concrete- Mechanism of Interaction and Remediation Strategy

FINAL REPORT  
JULY 2002

Submitted  
by

Farhad Ansari \*  
Professor and Head

Zhijun Zhang \*  
Ph.D Candidate

\* Dept. of Civil & Materials Engineering  
University of Illinois at Chicago  
Chicago, Illinois 60607-7023

Mr. Patrick Szary \*\*  
Research Engineer

Dr. Ali Maher \*\*  
Professor and Chairman

\*\* Dept. of Civil & Environmental Engineering  
Center for Advanced Infrastructure & Transportation (CAIT)  
Rutgers, The State University  
Piscataway, NJ 08854-8014



NJDOT Research Project Manager  
Mr. Nicholas Vitillo

In cooperation with

New Jersey  
Department of Transportation  
Division of Research and Technology  
and  
U.S. Department of Transportation  
Federal Highway Administration

## **Disclaimer Statement**

"The contents of this report reflect the views of the author(s) who is (are) responsible for the facts and the accuracy of the data presented herein. The contents do not necessarily reflect the official views or policies of the New Jersey Department of Transportation or the Federal Highway Administration. This report does not constitute a standard, specification, or regulation."

The contents of this report reflect the views of the authors, who are responsible for the facts and the accuracy of the information presented herein. This document is disseminated under the sponsorship of the Department of Transportation, University Transportation Centers Program, in the interest of information exchange. The U.S. Government assumes no liability for the contents or use thereof.

TECHNICAL REPORT STANDARD TITLE			
1. Report No. FHWA-NJ-2002-025	2. Government Accession No.	3. Recipient's Catalog No.	
4. Title and Subtitle Effects of Synthetic Air Entraining Agents on Compressive Strength of Portland Cement Concrete-Mechanism of Interaction and Remediation Strategy		5. Report Date July 2002	
		6. Performing Organization Code CAIT/Rutgers	
7. Author(s) Farhad Ansari, Zhijun Zhang, Ali Maher, and Patrick Szary		8. Performing Organization Report FHWA-NJ-2002-025	
9. Performing Organization Name and New Jersey Department of Transportation CN 600 Trenton, NJ 08625		10. Work Unit No.	
		11. Contract or Grant No.	
12. Sponsoring Agency Name and Federal Highway Administration U.S. Department of Transportation Washington, D.C.		13. Type of Report and Period Covered Final Report 2/1/2000-9/30/2001	
		14. Sponsoring Agency Code	
15. Supplementary Notes  <b>Acknowledgements</b>			
16. Abstract This report details the investigation pertaining to a research program which was undertaken in order to determine the reasons behind the loss of compressive strength in concretes containing synthetic air-entraining admixtures. The research program involved four different brands of admixtures, and two different types of admixtures per brand. The four brands are coded brands A, B, C, and D, respectively. A separate key to the brand codes is provided for NJDOT. Brand-C manufactured two different types of Vinsol resins and both were examined in this investigation. For brands B and D two types of mixtures were prepared: (1) those containing water reducing admixtures, and (2) mixtures with high range water reducers. While the primary objective of the research program was to investigate all the admixtures at normally recommended dosages, additional tests were performed for higher dosages for the agents manufactured by brand-D. The experimental program involved determination of compressive strength, measurement of air content at fresh state, detailed determination of air void parameters at the hardened state, and measurement of surface tension of admixtures in water and cement filtrates. The results of research indicated that, concretes produced by the synthetic air entraining admixtures, in general exhibited lower compressive strengths than those produced by Vinsol resin agents. The primary reason for the strength loss associated with the Synthetic air-entraining admixtures was creation of larger air bubbles (voids) by these admixtures. In general, synthetic air entraining admixtures increased the surface-tension-reduction capability of the cementitious mixture, giving rise to the creation of larger bubbles. However, results were brand sensitive and brand B synthetic agent exhibited not much of strength loss with good air void properties. Variable levels of strength loss were observed with other brands. Development of generalized correlation relationships between loss of strength and the use of synthetic agents will lead to erroneous results. It is possible to establish such relationships based on availability of data with information as to the brand, type,			
17. Key Words Portland Cement Concrete, Synthetic air-entraining Admixtures, Vinsol-Resin Admixtures, Air bubbles, Air Content, Air Void Parameters, Spacing Factor, Surface Tension, Compressive		18. Distribution Statement	
19. Security Classif. (of this report) Unclassified	20. Security Classif. (of this report) Unclassified	21. No. of 84	22. Price

Financial support from NJDOT to undertake this study is greatly appreciated.

## TABLE OF CONTENT

ABSTRACT .....	1
INTRODUCTION .....	2
BACKGROUND AND LITERATURE RESEARCH .....	2
Mechanism of Freeze-thaw Protection .....	3
Freezing of Cement Paste .....	3
Mechanism of Frost Attack and Protection .....	4
Fundamental Actions of Air-entraining Admixtures .....	6
Air-entraining Materials .....	6
Wood-Derived Products .....	8
Synthetic Detergents .....	9
Air-entrainment in mortar and concrete .....	9
The Entrained Air Void System .....	10
Behavior of Air-entrained Concrete In compression .....	12
Methods for the Determination of Air Content in Concrete .....	14
Gravimetric Method .....	14
Volumetric (Direct) Method .....	14
Pressure Method .....	14
Point Count Method .....	15
High-pressure Method .....	15
Linear Traverse Method .....	15
SUMMARY --- PHASE-I OBJECTIVES AND FINDINGS .....	16
OBJECTIVES AND SCOPE OF THE PRESENT RESEARCH (PHASE-II) .....	16
RESEARECH PROGRAM .....	17
Materials and Mix Proportions .....	18
Materials samples designation .....	18
Mix Procedures and Compressive Strength Tests .....	21
Air Void Analysis .....	22
Surface Tension Measurements .....	24
EXPERIMENTAL RESULTS .....	26
Series-I (WRA) .....	26
Series-II (HRWA) .....	32
Series-II at Higher Dosages of Air Entraining Admixtures .....	33
Surface Tension Test Results .....	33
ANALYSIS OF RESULTS .....	44
Series-I (WRA) .....	44
Series-II (HRWA) .....	45
Analysis of Surface Tension Data .....	60
Higher Dosages of Admixtures .....	63
CONCLUSIONS .....	66
RECOMMENDATIONS .....	68
APPENDIX-A: AUTOMATED LINEAR ANALYSIS SYTEM .....	69
Methodology .....	69

<b>Sample Preparation .....</b>	<b>69</b>
<b>Description of the system .....</b>	<b>72</b>
<b>System Reliability and Repeatability .....</b>	<b>73</b>
<b>APPENDIX-B: PENDANT DROP FOR SURFACE TENSION MEASUREMENT OF SOLUTION .....</b>	<b>76</b>
<b>REFERENCES .....</b>	<b>78</b>

## LIST OF FIGURES

Figure 1. Volume change occurring in cement pastes as the temperature is lowered. (Adapted from T.C. powers and R. A. Helmuth, Proceedings of the Highway Research Board, Vol. 32, 1953, pp.285-297) .....	4
Figure 2. Creation of hydraulic pressure in frozen cement paste. (a) non-air-entrained paste. (b) air-entrained paste. (Adapted from the Mindess and Young, Concrete, Prentice-Hall, Inc. New Jersey, 1981, pp564.) .....	5
Figure 3. Relationship between frost durability and bubble spacing factor of entrained air. (Adapted from the Mindess and Young, Concrete, Prentice-Hall, Inc. New Jersey, 1981, pp173) .....	6
Figure 4. Air-entraining agents attach air bubbles to cement particles.....	8
Figure 5. Effect of concrete parameters on total volume of entrained air. (Adapted from the Mindess and Young, Concrete, Prentice-Hall, Inc. New Jersey, 1981, pp176.).....	10
Figure 6. General relationship between capillary porosity and average strength of the various materials <sup>(6)</sup> (Adapted from G.J.Verbeck and R.A.Helmuth, Proceedings, Fifth International Symposium on the Chemistry of Cement, Tokyo, 1968, Vol. 3, pp1-32.) .....	13
Figure 7. Strength in relation to cement content for air-entrained and non-air-entrained concrete of constant slump (Adapted from Concrete Manual, 8th ed., U.S. Bureau of Reclamation, Denver, CO., 1975.) .....	13
Figure S1. Materials samples designation.....	18
Figure 8. MTS Materials testing system.....	22
Figure 9. Concrete slice sample preparation. (From left to right: lapping machine, slice after polishing, painting materials, sample ready for test) .....	24
Figure 10. Automated linear traverse system .....	24
Figure 11 Comparison of air void sizes for brand B admixtures (group-I measurements).....	48
Figure 12. Comparison of air void sizes for brand B admixtures (group-II measurements).....	48
Figure 13. Comparison of air void sizes for brand D admixtures (group-I measurements).....	49
Figure 14. Comparison of air void sizes for brand D admixtures (group-II measurements).....	50
Figure 15. Magnified image of air bubbles in VB.....	51
Figure 16. Magnified image of air bubbles in SB.....	51
Figure 17. Magnified image of air bubbles in VD1 (Magnification 52X).....	52
Figure 18. Magnified image of air bubbles in SD1 (Magnification 52X).....	52
Figure 19. Comparison of air void distributions in concretes produced with two different brands of synthetic air entraining admixtures (Series-I). .....	53
Figure 20. Comparison of air void size distribution for brand A admixtures (Series-II).....	53
Figure 21. Comparison of air void size distribution for brand B admixtures (Series-II).....	54
Figure 22. Comparison of air void size distribution for brand C admixtures	

(Series-II) .....	54
Figure 23. Comparison of air void size distribution for brand D admixtures (Series-II) .....	55
Figure 24. Magnified images of air bubbles in SVB and SSB (Magnification 52X) .....	56
Figure 25. Magnified images of air bubbles in SVD1 and SSD1 (Magnification 52X) .....	57
Figure 26. Magnified images of air bubbles in SVA and SSA (Magnification 52X) .....	58
Figure 27. Magnified images of air bubbles in SVC1, SVC2 and SSC (Magnification 52X) .....	59
Figure 28. Surface tension of air entraining agent in water solution.....	62
Figure 29. Surface tension of filtrate of cement paste.....	62
Figure 30. Surface tension of Brand-D water solution.....	64
Figure 31. Surface tension of Brand-D filtrate of cement paste .....	64
Figure 32. Typical surface image of samples SVD2 and SSD2 .....	65
Figure 33. Typical surface image of samples SVD3 and SSD3 .....	66
Figure 34. Concrete surface after proper lapping (1) .....	70
Figure 35. Concrete surface after proper lapping (2) .....	70
Figure 36. Concrete surface after proper painting (1) .....	71
Figure 37. Concrete surface after proper painting (2) .....	71
Figure 38. Configuration of system .....	72
Figure 39. View of computer screen .....	73
Figure 40. Repeatability test (1) .....	75
Figure 41. Repeatability test (2) .....	75
Figure 42. (Left) Geometry and notation of symbols of a pendant-drop profile ...	76

### **LIST of TABLES**

Table 1 .Characteristics of air-entrained concrete at optimum frost resistance (cement content 250lbs/yd <sup>3</sup> , or 326kg/SVB).....	11
Table 2. Coarse aggregate sieve analysis (22 lb. sample) .....	18
Table 3. Fine aggregate sieve analysis (1.1 lb. sample) .....	19
Table 4. Concrete mix design (Series-I).....	19
Table 5. Concrete mix design (Series-II).....	19
Table 6. Concrete mix designation according to air-entraining admixtures (Series-I) .....	20
Table 7. Concrete mix designation according to air-entraining admixtures (Series-II).....	21
Table 8 . Surface tension sample designations, dosages, and densities (water solution) .....	25
Table 9. Surface tension sample designations, dosages, and densities (filtrate of cement paste) .....	26
Table 10. Compressive strength and air content for series-I experiments (Groups	



I and II).....	27
Table 11. Parameters of measured air-void system in hardened state (Series-I, Group-I) .....	28
Table 12. Parameters of air-void system in hardened state (Series-I, Group-II) .....	28
Table 13. Comparison of air void distribution for VB and SB (Series-I Group-I) .....	29
Table 14. Comparison of air void distribution for VD1 and SD1 (Series-I Group-I) .....	30
Table 15. Comparison of air void distribution for VB and SB (Series-I Group-II) .....	31
Table 16. Comparison of air void distribution for VD1 and SD1 (Series-I Group-II) .....	32
Table 17. Compressive strength and air content for series II specimens.....	34
Table 18. Parameters of air-void system in hardened state for series II specimens.....	35
Table 19. Comparison of air void distribution for SVA and SSA (Series II) .....	36
Table 20. Comparison of air void distribution for SVB and SSB (Series II) .....	37
Table 21. Comparison of air void distribution for SVC1, SVC2 and SSC (Series II) .....	38
Table 22. Comparison of air void distribution for SVD1 and SSD1 (Series II).....	39
Table 23. Specimen designations, compressive strengths and the air contents for samples produced through additional dosages of brand-D admixtures .....	40
Table 24. Comparison of air void distribution for SVD2 and SSD2 .....	41
Table 25. Comparison of air void distribution for SVD3 and SSD3 .....	42
Table 26. Parameters for measured air-void system of samples with additional dosage for Brand-D admixtures .....	43
Table 27. Surface tension measurement result (dyne/cm).....	43
Table 28. Surface tension of solutions with Brand-D admixtures at higher dosages of air entraining admixtures .....	43
Table 29. Results from automated tests are Comparable to ASTM C 457 .....	74

## ABSTRACT

This report details the investigation pertaining to a research program which was undertaken in order to gain knowledge as to the reasons behind the loss of compressive strength in concretes containing synthetic air-entraining admixtures. The research program involved four different brands of admixtures, and two different types of admixtures per brand. The four brands are coded brands A, B, C, and D, respectively. A separate key to the brand codes is provided for NJDOT. Brand-C manufactured two different types of Vinsol resins and both were examined in this investigation. Therefore, altogether, five types of Vinsol resin and four types of synthetic admixtures were investigated. While the primary objective of the research program was to investigate all the admixtures at normally recommended dosages, additional tests were performed for higher dosages for the agents manufactured by brand-D. The experimental program involved determination of compressive strength, measurement of air content at fresh state, detailed determination of air void parameters at the hardened state, and measurement of surface tension of admixtures in water and cement filtrates. The results of research indicated that, concretes produced by the synthetic air entraining admixtures, in general exhibited lower compressive strengths than those produced by Vinsol resin agents. The primary reason for the strength loss associated with the Synthetic air-entraining admixtures was creation of larger air bubbles (voids) by these admixtures. Examination of brand-D at higher dosages further confirmed the existence of correlation between the surface tension, bubble size distribution in hardened concrete and compressive strength. In this case, increased levels of Vinsol resin admixtures was associated with strength loss, whereas, increasing the dosage of synthetic admixtures, first increased the compressive strength and then reduced it.

In general, synthetic air entraining admixtures increased the surface-tension-reduction capability of the cementitious mixture, giving rise to creation of larger bubbles. The results reported here do not preclude the use of synthetic agents for entrainment of air in concretes. However, it seems that the interaction between cementitious mixtures and synthetic air entraining admixtures are not quite understood and more data is needed for proper proportioning of the synthetic admixture in concretes. A major ramification of the research conducted in this study was direct correlation between decrease in the surface tension of cement filtrate and the strength loss (due to larger bubbles). A simple test is proposed where cement filtrate of the exact water-cement ratio is used for the determination of the surface tension of the expected mixture. This test could be employed to predict the behavior of certain air-entraining admixtures, prior to the application in the field, i.e. pavements.

## **INTRODUCTION**

This report pertains to the research performed during the second phase of the study investigating the effects of synthetic air entraining agents on the compressive strength of Portland cement concrete. A final report corresponding to the results obtained during the first phase of the study has already been submitted to NJDOT. For completeness, a short summary of the first phase findings will be outlined immediately following the introduction section of this report.

Nearly all of the concrete employed in construction is air entrained. Besides improving freeze-thaw durability, air entraining increases the workability of concrete, and therefore allows for a reduction in water to cement ratio ( $w/c$ ). The lower  $w/c$  ratio that can be achieved with air-entrained concrete and better compaction characteristics results in more impermeable concrete and a better overall resistance to aggressive agents. However, introduction of additional void space with air entrainment will have a detrimental effect on strength. A strength loss of 10 to 20 % can be anticipated for most air-entrained concretes. This reduction in strength is anticipated and is compensated for during mix proportioning of concrete by reducing the amount of required sand and water. Water content can be generally reduced by 30 to 50 lbs/yd<sup>3</sup> for a 5% increase in air content. This partially offsets the strength reduction that accompanies air entrainment.

Recent experience of NJDOT with synthetic air entraining admixture has indicated statistically a rather large decrease in strength. An average bias of 700 lbf/in<sup>2</sup>, 600 lbf/in<sup>2</sup> and 300 lbf/in<sup>2</sup> has been estimated with Class A, Class B White and Class B concrete respectively. According to NJDOT observations, this decrease in strength has been isolated independently of parallel contributions from varying air content, ambient temperature, Portland cement quality control and differing alkali contents in Portland cement. Such losses in strength were not observed with Vinsol resin type air entraining agents. Therefore, the mechanism of strength loss in concretes with entrained air bubbles from synthetic air entraining agents has not been understood.

Much research has been done on the subject of air entrainment, specifically as it pertains to the mechanisms of freeze-thaw action in concrete; protection by entrained air system; and air entraining admixtures and mechanism of bubble formation. Research results have been documented in various technical articles, and summarized in a number of excellent books including the books by T.C. Powers<sup>(1)</sup>, S.M. Mindess, and J.F. Young<sup>(2)</sup>. The introduction section of this report includes direct excerpts and relevant figures from these fine books.

## **BACKGROUND AND LITERATURE RESEARCH**

According to T.C. Powers,<sup>(1)</sup> the practice of deliberately entraining air bubbles in

concrete was dated back to 1930's, and it has since become one of the most important developments in modern concrete technology. Entrainment of air is accomplished by use of a suitable agent, which stabilizes bubbles formed from some of the air incorporated during the mixing process. One of the major disadvantages of traditional concrete is its susceptibility to damage during freezing and thawing cycles when it is exposed to saturated condition. Concrete can be badly damaged after a single winter's exposure if corrective measures are not taken, and this rapid deterioration precludes the use of concrete in most major applications: highway pavement, foundations of huge structures, and dams. The practice of using entrained air in concrete has in general been highly successful, but there are exceptions. Full comprehension of the research approach undertaken during this investigation requires a brief description as to the mechanisms of air entrainment, and the testing procedures for determination of air content and air bubble characteristics in concrete. This is accomplished in this section of the report.

### **Mechanism of Freeze-thaw Protection**

It is well known that porous materials containing moisture are susceptible to damage under repeated cycles of freezing and thawing (frost attack). Hardened concrete paste, which has a high porosity, is particularly susceptible to such conditions, and concrete may be fairly destroyed in a winter in northern climates. Fortunately, air entrainment has proved to be an effective and reliable means of protecting concrete from frost attack. It is of interest to examine the mechanism by which damage occurs on repeated freezing and thawing and thereby determine the critical factors affecting frost resistance and the reasons why air entrainment is effective. <sup>(2)</sup>

### **Freezing of Cement Paste**

When saturated concrete is cooled to below 0°C, immediate freezing of most of the water in the cement does not occur. The fact is that paste contains a wide spectrum of pore sizes, and it can be shown thermodynamically that water in capillary pores will not freeze until the temperature is lowered below 0°C by an amount that depends on the diameter of the pore. According to S. Mindess and J. F. Young, "*water in pores of 10nm diameter will not freeze until -5°C (23°F), and in pores of 3.5nm diameter water will not freeze until -20°C (-4°F).* Furthermore, *water absorbed on the surfaces of C-S-H (calcium silicate hydrate), which forms the surfaces of capillary pores and also creates micropores within the paste, will never freeze, although it may migrate to the capillary pores, where it can freeze*". It has been shown that in an unprotected paste severe dilation accompanies freezing (figure 1), which leads to internal tensile stresses and cracking. In an air-entrained paste, very little dilation occurs and considerable shrinkage during freezing is observed at low temperature. <sup>(2)</sup>

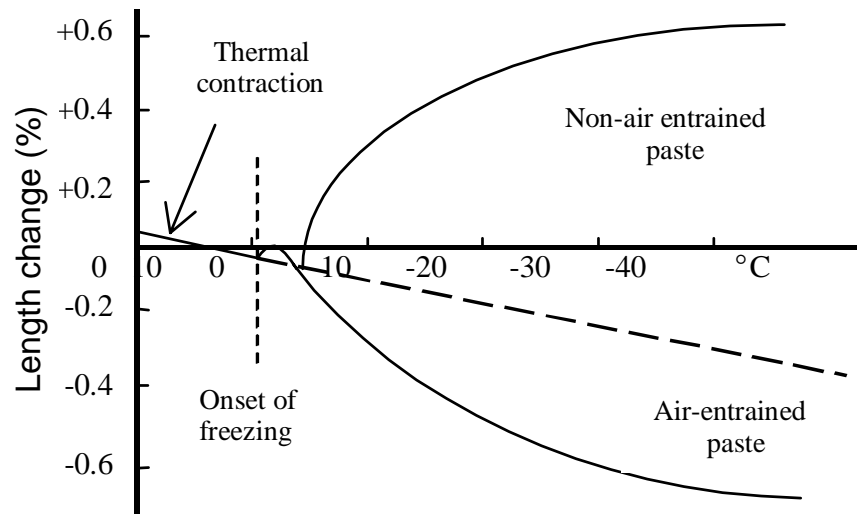


Figure 1. Volume change occurring in cement pastes as the temperature is lowered. (Adapted from T.C. powers and R. A. Helmuth, Proceedings of the Highway Research Board, Vol. 32, 1953, pp.285-297)

### **Mechanism of Frost Attack and Protection**

Several different processes can contribute to paste behavior during freezing. These processes could be generation of hydraulic pressure by ice formation, desorption of water from C-S-H gel, and so on. Although there is 9% volume increase accompanied with the freezing of water, this change is insufficient to account for all of the dilation observed in cement paste and in concrete. Some of the dilation that occurs on freezing is probably due to direct expansion of ice in microcracks, and this will increase if progressive microcracking occurs during continued freezing and thawing.

The major dilation that occurs is attributed to the generation of hydraulic pressure. According to Young and Mindess, *“As ice forms in a capillary, the accompanying volume increase causes the residual water to be compressed. This pressure can be relieved if the water can escape from capillary to a free space by diffusing through unfrozen pores, but if the water has too far to move to an escape boundary, the capillary will tend to dilate and the surrounding material will come under stress (figure 2). The superposition of pressure from adjacent capillaries will eventually cause the tensile strength of the paste to be exceeded and rupture will occur. As the temperature is progressively lowered, more capillary water is involved in freezing, increasing the hydraulic pressures and thereby increasing microcracking and dilation. In a saturated non-air-entrained paste, the only free space is the exterior of the specimen, and the diffusion of water to the outside is too slow to relieve the hydraulic pressure. Thus, the inclusion of entrained air provides empty space within the paste to which the excess water can move and freeze without damage”*. The bubbles act as “safety valves” and the spacing factor determines the average distance the water must

travel to reach the free space. This distance must not be too great if hydraulic pressure is to be relieved; hence the requirement of a critical spacing factor. <sup>(2)</sup>

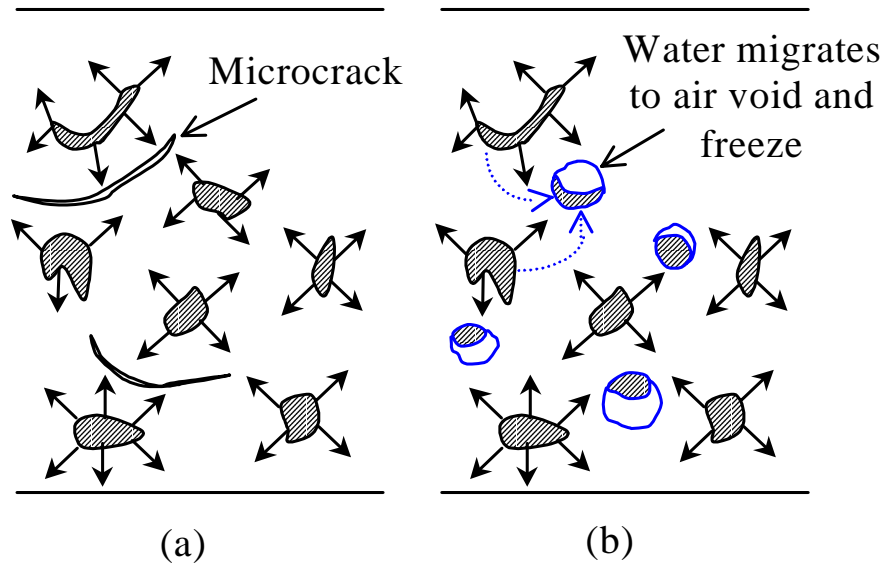


Figure 2. Creation of hydraulic pressure in frozen cement paste. (a) non-air-entrained paste. (b) air-entrained paste. (Adapted from the Mindess and Young, Concrete, Prentice-Hall, Inc. New Jersey, 1981, pp564.)

It can be shown that the resistance to freezing and thawing depends on the permeability, the degree of saturation of paste, the amount of freezable water, the rate of freezing, and the average maximum distance from any point in the paste to a free surface where ice can form safely. Therefore, the use of air-entraining admixture to entrain a sufficient volume of air bubbles (typical ~4-8%), which are small enough and uniformly dispersed to achieve reasonable spacing (figure 3), is the most efficient means for achieving frost durability.

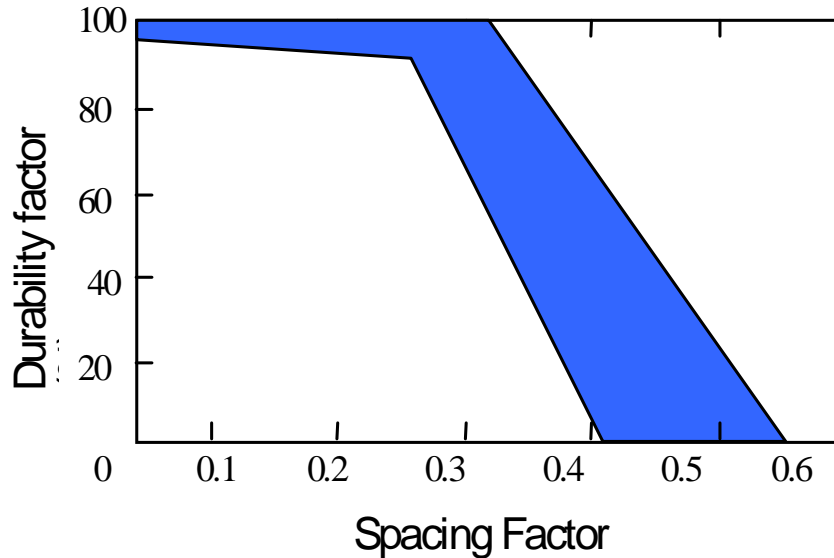


Figure 3. Relationship between frost durability and bubble spacing factor of entrained air. (Adapted from the Mindess and Young, Concrete, Prentice-Hall, Inc. New Jersey, 1981, pp173)

### **Fundamental Actions of Air-entraining Admixtures**

Air-entraining mixtures do what their names suggest: they entrain or retain air in the concrete. They must contain compounds that will promote the formation of stable foam. Bubble formation in water is normally a transient phenomenon because the high surface tension of water opposes the creation of the air-water interface that bound a bubble. Foams can only be formed if the energy barrier represented by surface tension can be overcome in order that masses of bubbles can be created during agitation. However air bubble entrainment is a fairly complicated chemical as well as physical procedure, the following several paragraphs are dedicated to the discussion of this paradigm.

### **Air-entraining Materials**

Air-entraining agents contain surface-active agents which concentrate at the air-water interface, lower the surface tension so that bubbles can form more readily, and stabilize the bubbles once they are formed. Surface-active agents are molecules, which at one end have chemical groups that tend to dissolve in water (hydrophilic group), and which at the other end have groups that are repelled by water (hydrophobic group). The molecules tend to align at the interface with their hydrophilic groups in the water and the hydrophobic groups in air at solid-water interface, when special directive forces exist on the solid surface. Surface-active molecules are specially adsorbed with the hydrophilic group bound to the solid and the hydrophobic group oriented towards the water. <sup>(3)</sup> This phenomenon makes the solid surface-hydrophobic so that air may displace water from it and,

as a consequence, air bubbles may adhere to the solid (figure 4). Carboxylic acid or sulfonic acid groups are commonly responsible for the hydrophilicity of the molecules, while aliphatic or aromatic hydrocarbons make up the hydrophobic component. Air-entraining admixtures are thus closely related to synthetic detergents, although the foaming capacity of the latter is only a side effect of other “surface-active” properties.

Surface-active agents can be classified according to the type of polar (hydrophobic) group in their molecules: <sup>(4)</sup>

- Anionic agents: the most used anion is sulphates, sulphonated hydrocarbons, sulphonates esters and carboxylates. The most commonly used cations are  $\text{Na}^+$ ,  $\text{NH}_4^+$  and triethanolammonium and  $\text{NH}^+(\text{C}_2\text{H}_4\text{OH})_3$ . Neutralized Vinsol resin falls in this class.
- Cationic agents, e.g. alkylamine hydrochlorides  $\text{RNH}_3^+\text{Cl}^-$  and alkyl trimethyl ammonium bromides  $\text{RN}(\text{CH}_3)_3^+\text{Br}^-$  where R is an alkyl group.
- Non-ionic agents: the most frequently encountered nonionic surfactants are Non-nitrogenous, Alkanolamides and polymers of alkylene oxides, for example, polyethylene glycol esters  $\text{RCO}(\text{OC}_2\text{H}_4)_n\text{OH}$ , dialkanolamides  $\text{RCON}(\text{C}_n\text{H}_{2n}\text{OH})_2$ .
- Amphoteric agents: both the acid and the basic groups of amphoteric type surfactant can be either weak or strong, four classes of commonly used amphoteric, without considering those with more than one functional group of one type or the other, are distinguished as Carboxylates with weakly basic, Carboxylates with strong basic, Sulphonates (sulphobetaines) with weakly basic, and Sulphonates (sulphobetaines) with strong basic.

However, commercially available air-entraining agents are usually manufactured from chemically complex raw materials, and the final products may contain blends of these raw materials plus other raw materials or chemicals, thus it is difficult to define air-entraining agents chemically except by rather broad classification. Wood-derived products and synthetic detergent, two types of most frequently used air-entraining agents, are described here. <sup>(5)</sup>



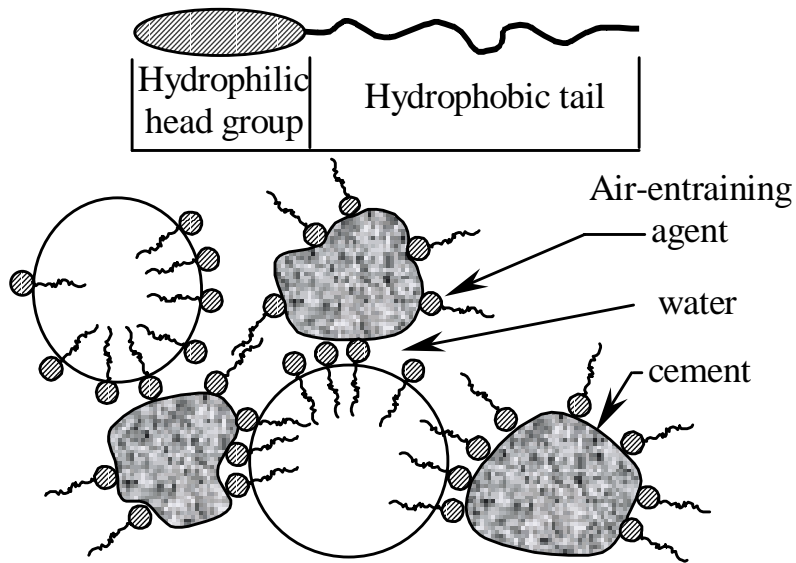


Figure 4. Air-entraining agents attach air bubbles to cement particles

### ***Wood-Derived Products***

In the first few decades after the introduction of air-entraining agents for concrete, the most widely used products were based on neutralized Vinsol resin, this material is derived as a by-product of a process for recovering various solvents and rosins from pine wood. After series extractions with hydrocarbons, an insoluble residue remains, these were later trademarked as Vinsol resin. This resin is highly complex, made up of approximately 60 percent phenolic compounds, 15 percent waxes and terpenes, and the remainder as resin acids. In order to function as a concrete admixture it is converted to soluble form by neutralization with sodium hydroxide to form the soluble sodium soap. This neutralization allows the admixture to begin to form films around air bubbles immediately after addition to and subsequent agitation of the concrete mix, as it does not require any further reaction with alkalis generated by cement hydration. For this reason, entrained air is generated quickly with Vinsol resin based air entraining agents, and there is temporary minor air gain with continued mixing, followed by air loss with prolonged mixing. It is claimed that the air bubble present in air-entrained concrete produced with NVR tend to be mid-sized as compared to those from other groups of air-entraining agents.

Manufactures have turned to other raw materials, which are also by-products of wood processing and are chemically similar to NVR. While wood derivatives (such as tricyclic acids) are a primary constituent of these materials, as with NVR, a minor amount of fatty acids may also be present. The properties, dosage rate, and performance of these materials are similar to that of NVR.

Another group of materials derived from wood processing is the tail oil. These contain fatty acids, characterized by a long hydrocarbon chain which terminates

in a carboxylic (-COOH) end group. These include the unsaturated oleic acid, and saturated acids with chain lengths of 8 to 18 carbon atoms, such as capric acid (C<sub>9</sub>). These compounds generate air more slowly than NVR, and air may tend to increase with prolonged mixing as more of the acids react with alkalis generated during cement hydration. These agents appear to generate the smallest air bubbles of any of the currently available air-entraining agents.

### ***Synthetic Detergents***

In Industrial process used for production of lubricating oils and kerosene, aromatic sulfonic acids are produced as by-products and exhibit excellent detergent characteristics. Water-solution fractions of these compounds are removed from the residues and consist generally of aryl-alkyl sulfonates. Such sulfonates can also be neutralized with caustic soda to form water-soluble sodium sulfate. Compounds of this class which have been used to produce air-entraining agents include ortho- and para-sodium dodecyl benzene sulfonate and sodium dodecyl sulfate. While synthetic detergents allow for quick generation of air bubbles in concrete, these bubbles tend to be coarser than those produced using wood-derived materials. While their primary application has been for foaming agents, some are also used as air-entraining agents. The synthetic detergents have been blended with water-reducing agents to produce water-reducing /air-entraining agents, but these are not marketed in the United States.

### **Air-entrainment in mortar and concrete**

The air-entraining potential of an admixture depends on the concrete materials used and their proportions. Finely ground cements entrain less air than do more coarsely ground ones. The gradation and particles shape of the aggregates will also affect air. Impurities in water may have positive or negative effects on air entrainment. The use of other admixture simultaneously with air-entraining agents should be approached with caution, because they may affect air-entraining abilities. Calcium chloride can be used successfully, but some common chemical admixtures may interact when mixed with air-entraining admixtures and inhibit entrainment. In such case the second admixture should be added to the concrete after the air has been entrained. Cement content has a marked effect on the total air entrained. At a given dose, lean concretes entrain more air than more rich mixes, and low w/c ratio concretes entrain less air than concretes with high w/c ratios. Other factors governing the air entrainment are mixing and consolidation. The total volume of entrained air depends on the type of mixer, the rate of mixing, and the amount of concrete being mixed. The time of mixing is also important: the air content will initially increase with time and then gradually decrease during prolonged mixing. Maximum air entrainment is generally achieved during normal mixing time. Temperature is also an important parameter that affects air entrainment: air content varies inversely with temperature. Increasing the temperature from 50°F to 100°F will approximately halve the air content. Vibration significantly reduces the air contained in concrete too (Figure 5).<sup>(2)</sup>

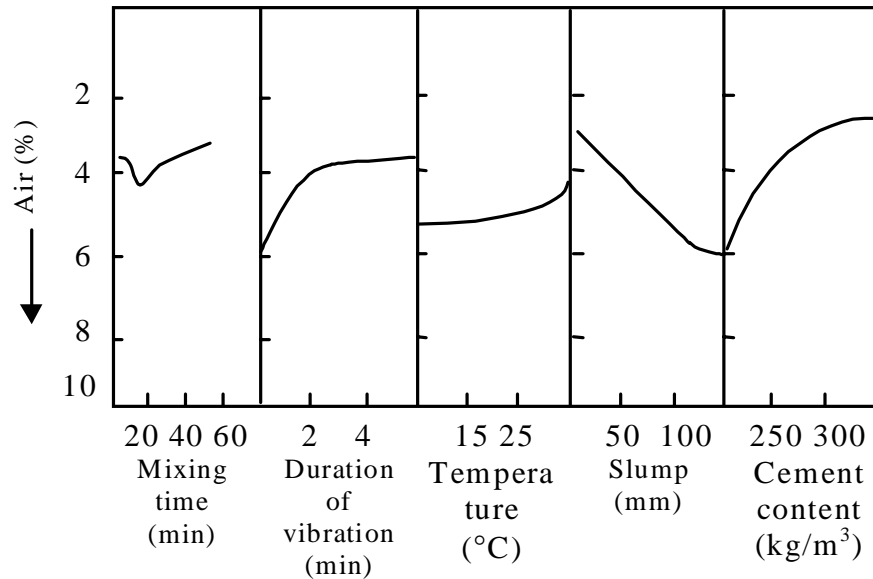


Figure 5. Effect of concrete parameters on total volume of entrained air. (Adapted from the Mindess and Young, Concrete, Prentice-Hall, Inc. New Jersey, 1981, pp176.)

For the given materials, mixing and consolidation, the entrained air void characteristics is dominated by the air-entraining capacities of surface-active agents in mortar and concrete. Although it is generally accepted that the lower the surface tension of the surface-active agents, the greater the air-entraining capacities, the complexity of the chemical interaction between surface-active agents and cement indicate that the story could be different for different admixtures. G.M.Brueere made a series of surface tension measurements in surface-active agent solution and in filtrate from cement pastes containing surface-active agent, in an attempt to correlate surface tension lowering with entrained air void characteristics. <sup>(3)</sup> Solution of mixtures of dodecyl alcohol and sodium dodecyl alcohol were shown to have lower surface tension than solution of sodium dodecyl sulphate, and when solutions were shaken in stoppered cylinders the mixed agents were observed to produce foams consisting of bubbles with smaller size than those produced by sodium dodecyl sulphate. However, the surface tensions of filtrates from paste containing the mixed agents were higher than those in filtrates from paste containing sodium dodecyl sulphate alone. Thus the correlation between surface tension lowering and mean bubble size found in aqueous solutions does not hold for paste filtrates and entrained bubbles in paste. The effects of agent types on the bubble size characteristics in pastes mixed under equal conditions could not be explained from the data available at the time.

### The Entrained Air Void System

The principal purpose of entraining air in concrete can be accomplished by

providing a sufficiently large number of bubbles per unit volume of paste to produce a cellular structure in which the cell walls, composed of hardened paste, are only a few thousands of an inch thick. For a given percentage of air, the smaller the average thickness of the walls between bubbles is, the smaller the mean bubble diameter and hence the larger the number of bubbles, therefore, we are concerned not only with the quantity of the entrained air, but also with the characteristics of the air void system, particularly the bubble size distribution, spacing factor and specific surface area.

The volume of air required to give optimum frost resistance has been found to be about 9% by volume of the mortar fraction, or practically 4-8% by volume of concrete. Most of the entrained air are greater than 0.0004 inches (10µm) and less than 0.05 inches (1.25 mm) in diameter and are uniformly distributed throughout the concrete. The critical parameter of the air-entrained paste is the spacing factor, which is defined as the average maximum distance from any point in the paste to the edge of a void. The spacing factor should be around 0.2mm (0.008 inches) to ensure adequate frost protection, the smaller the spacing factor, and the more durable the concrete (table 1).

Table 1 .Characteristics of air-entrained concrete at optimum frost resistance (cement content 250lbs/ycd3, or 326kg/SVB)1

Measured air content (% by volume)					
maximum aggregate size mm (in.)	non-air-entrained	recommended air content (ACI) ±%	concrete	paste	bubble spacing factor mm (in.)
63.5 (2 1/2)	0.5	4.0	4.5	16.7	0.18 (0.007)
38 (1 1/2)	1.0	5.0	4.5	16.4	0.20 (0.008)
19 (3/4)	2.0	6.0	5.0	16.9	0.23 (0.009)
9.5 (3/8)	3.0	7.5	6.5	19.7	0.28 (0.011)
mortar	---	---	---	23.0	0.30 (0.012)

Furthermore, small voids remain as discrete, isolated bubbles which do not readily fill with water even when the concrete is kept saturated. Since void sizes are not uniform, they are expressed in terms of specific surface ( $\text{mm}^2/\text{mm}^3$  of concrete); typically, values should be in the range of 16 to 25  $\text{mm}^{-1}$  (400 to 625  $\text{in}^{-1}$ ).<sup>(2)</sup>

<sup>1</sup> Based on data from Klieger, in significance of Tests and Properties of Concrete and Concrete-Making Materials, ASTM STP 169 B, pp.787-803, American Society for Testing and Materials, Philadelphia, PA, 1978.

## Behavior of Air-entrained Concrete In compression

The primary factor that governs the strength of brittle materials is porosity. A number of models have been proposed to describe the basic strength-porosity relationship. The most commonly adapted model with a reasonably good fit to the experimental data well over a wide range of porosities in many systems, is the exponential expression <sup>(2)</sup>

$$S = S_0 e^{-kp} \quad (1)$$

Where S is the strength,  $S_0$  the strength at zero porosity (“intrinsic strength”), p the fractional porosity, and k a constant that depends on the system being studied. This equation and many others that have been proposed represent a considerable simplification of the system. The nature of the material, the size and the shape of the pores, and whether the pores are empty or filled with a fluid all must have some effect. Nevertheless, whatever the best form the strength-porosity relationship takes for a particular system, it is clear that strength depends mainly on the porosity. Figure 6 presents such a curve, with the plotted data representing a number of normally cured cements, more crystalline autoclaved cements, and a variety of aggregates.

Figure 7 illustrates the effect of entrained-air voids and cement content on the compressive strength of concrete. With entrained air, the strength of concrete is usually less than that of similar concrete without air. In general terms, given that the concrete mixtures are properly compacted and the slump is kept constant, we can expect a 5 percent loss of strength for each percentage point of air content added to the concrete. However, this may vary significantly, and can actually range from about 2 to 6 percent depending on the particular mix. For the low-cement content mixes, as shown in Figure 7, there is a slight improvement in strength since the strength reduction by incorporating air is mostly offset by the reduced water content to maintain the same slump. Therefore, the effect of air in reducing strength is more significant with higher cement factor mixtures.

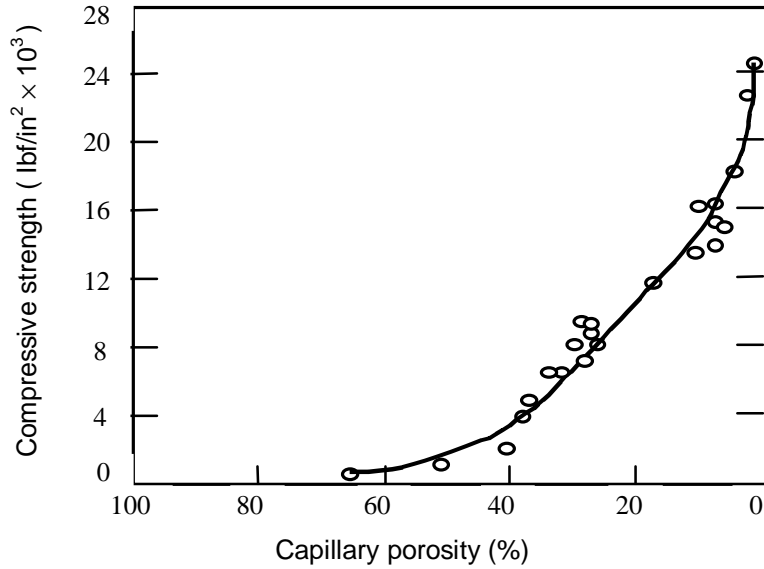


Figure 6. General relationship between capillary porosity and average strength of the various materials <sup>(6)</sup> (Adapted from G.J.Verbeck and R.A.Helmuth, Proceedings, Fifth International Symposium on the Chemistry of Cement, Tokyo, 1968, Vol. 3, pp1-32.)

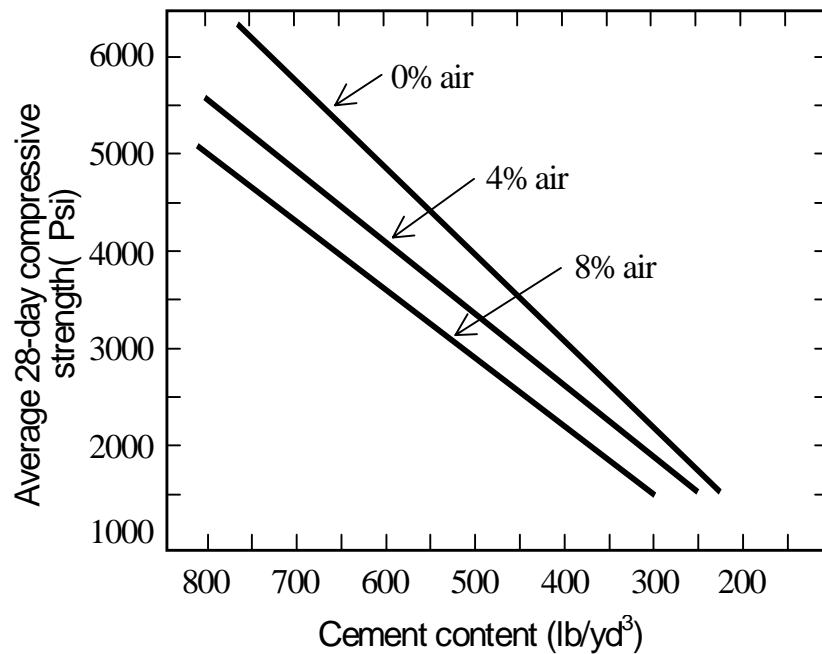


Figure 7. Strength in relation to cement content for air-entrained and non-air-entrained concrete of constant slump (Adapted from Concrete Manual, 8th ed., U.S. Bureau of Reclamation, Denver, CO., 1975.)

As in other brittle materials, the fracture and failure process in concrete must pass through three stages: crack initiation, slow (subcritical) crack growth, and dynamic crack propagation which lead to the failure of material. Besides the crack arresting action of aggregate or branching action of microcracking, crack propagation is also deferred by the entrainment of uniformly distributed air bubbles. In air-entrained matrices, cracks travel around the air bubbles and therefore deferring the propagation. This action has been well known in homogenous materials and to what extent it affects the strength of concrete still remains unknown.

## **Methods for the Determination of Air Content in Concrete**

A number of techniques are available for the determination of air content in fresh or hardened state. These methods include the following: <sup>(1)</sup>

### **Gravimetric Method**

The air content of fresh concrete can be calculated from its measured unit weight and from the weights and densities of its ingredients. This procedure is standardized by ASTM(C 138). This technique is highly accurate provided the densities of concrete constituents are accurately determined. Time required for measurement of air varies depending on whether the accurate unit weight of constituents are available or they need to be measured. Time required vary from 45 minutes to about 2 hours.

### **Volumetric (Direct) Method**

The volumetric or direct method is based on determining the air content of fresh concrete by removal of the air from a measured volume of concrete and measurement of the volume of air directly. This method, originated by Pearson and developed by Menzel, is described in ASTM Designation C 173. It involves mixing a volume of concrete with a similar volume of water in a closed container designed to serve as a picnometer. The separate volumes of concrete and water at first fill the container, but after mixing the extra water and concrete by shaking and rolling the container, air in the concrete become released and collected in the top calibrated part of the container. That part of the total air content that was held in porous rock particles is mostly retained by the particle. The instrument for performing this process is called a Roll-A-Meter. Time required for proper measurement of air content is about 45 minutes.

### **Pressure Method**

Introduced by Klein and Walker in 1946, this method is based on Boyle's law: At a given temperature the volume of a given mass of air varies inversely with pressure applied to the air, provided that the pressure are not much above 1 atm.

Since air is the only appreciably compressible ingredient of concrete, any reduction in the volume of a sample of fresh concrete due to an increase of external pressure may be ascribed to the air in the specimen. By increasing pressure on a sample in a closed container, and measuring the resulting decrease of volume, the quantity of air in the sample can be calculated.

Any air held in the pore within permeable rock particles is included in the calculated amount, and since air so situated is not considered the subject of control procedure, the gross amount is subject to correction factor. To establish the correction factor, it is necessary to treat a sample of inundated aggregate in the same way as the concrete, thus ascertaining the air content of the particles composing the aggregate. Use of an oven-dried sample, for example, even after prolonged soaking, might contain a different amount of air than does the same material as received from pit or quarry. The ASTM designation for this technique is C 231.

### **Point Count Method**

This is a method for determination of air content on hardened concrete. It is based on statistical considerations and requires a finely ground plane cross-section of the specimen. In this procedure, a rectangular grid is placed on the plane specimen surface, and each grid intersection that falls within a void section is counted. The air content is equal to the number of such coincidence with voids divided by the total number of grid intersections.

In practice the grid is created optically, point by point, by means of a mechanical stage capable of bilateral stepwise movements, mounted under a fixed binocular microscope. In typical use the stage is moved laterally by equal steps of about 0.05 inch for a distance of at least 5 inch, counting the total number of steps, and the number of times the index point in the reticule of one of the eyepieces is seen to be within the boundary of a void section. Such traverses are repeated on parallel lines about 0.2 inch apart until the grid is complete. The ASTM designation for this method is C 457.

### **High-pressure Method**

Introduced by Lindsay, the high pressure method is also applicable to hardened concrete. It involves compressing the air in an oven-dried and presoaked specimen by means of hydraulic pressure, but instead of applying about 10 lbf/in<sup>2</sup> as for fresh concrete, a pressure of 5000 lbf/in<sup>2</sup> is used. After applying correction factors, a value for air content is obtained which, according to Erlin<sup>(7)</sup>, is in good agreement with that given by the pressure method applied to fresh concrete. This technique has not gain wide spread usage.

### **Linear Traverse Method**

The linear traverse method pertains to the measurement of air content in



hardened concrete. It involves slicing the specimen, polishing the cut surface, and measuring the fraction of the total area occupied by sections of air bubbles. By using this technique, important information about the air void characteristics of the sample can be determined. This information includes air bubble size, distribution, spacing, and total air content. ASTM designation for this method is C 457.

## **SUMMARY --- PHASE-I OBJECTIVES AND FINDINGS**

The primary objective of the research reported during the first phase of the project was to investigate the cause and the mechanism for reduction in compressive strength when Synthetic air entraining admixtures are used. The investigation involved comparison of the compressive strengths of concretes entrained with air bubbles from synthetic and Vinsol resin type admixtures. The scope of the study pertained to a single brand for both admixture types. The experimental program included determination of air content and other rheological properties at the fresh as well as hardened states. An automated linear traverse system based on image processing protocols was employed for the characterization of air bubbles in the hardened state. The air bubble distribution of the Synthetic and Vinsol resin mixtures at the same air content were compared and correlated against their respective strengths. Comparison of results indicated that Vinsol resin admixture produced more of the smaller bubble sizes desirable for protection against frost. In fact, comparison of air bubble size count revealed that the main reason for higher air contents in Synthetic mixtures was due to the increased number of larger air bubbles within the cement paste. Detailed experimental data and analysis of results can be found in the first phase final report. Although, these results were conclusive with one brand of admixture, it was decided not to generalize the findings until a more comprehensive analysis was performed involving most of the admixture brands commonly employed in the North America. Therefore, the second phase of this project was commenced to investigate the compressive strength loss phenomenon with these brands.

## **OBJECTIVES AND SCOPE OF THE PRESENT RESEARCH (PHASE-II)**

Phase-I research results were significant in that the cause and mechanism of strength loss was clearly attributed to the larger air bubble sizes in concretes entrained with synthetic admixtures. Moreover, this project and the demand for petrographic analysis of many concrete samples led to the development of an automated image analysis system. The correlation between the bubble size and strength loss led the research team to deduce that the “surface tension” reduction capabilities of the synthetic admixtures may be the main cause for the strength loss in concrete. Bubble formation is physically attributed to surface tension of the phase in the paste/liquid stage. Air entraining agents contain surface-active agents that concentrate at the air-water interface, lower the

surface tension so that bubbles can form more readily, and stabilize the bubbles once they are formed. The larger air bubble sizes in synthetic admixture concretes suggests that these admixtures reduce the surface tension more markedly than do their Vinsol resin counterparts. Would this hypothesis hold for all the admixture brands? Moreover, do the strength losses observed with first phase experiments hold for all different brands of the synthetic admixture concretes, or will the different brands behave differently?

In responding to these questions, the primary objectives of the phase II project were:

- (1) To investigate the strength loss, and compare the compressive strengths of synthetic and Vinsol resin type admixtures for all the prevailing admixture brands.
- (2) Based on the hypothesis stated earlier, perform surface tension measurements in order to pinpoint the exact nature of the interaction between synthetic admixtures and Portland cement concretes.

## **RESEARECH PROGRAM**

The general overview of research program is briefly described here. To achieve the stated objectives of the research, the experimental program included the following tests, analysis, and measurements:

1. Compressive Strength Tests.
2. Air void analysis.
3. Surface tension measurements.

Four different brands of air entraining admixtures, namely: Brand-A, Brand-B, Brand-C, and Brand-D were employed in the study. A key for the four brands is submitted as an addendum to this report. Both Synthetic and Vinsol resin types of admixtures per manufacturer were examined. In the case of the Brand-C, two types of Vinsol resin-based admixtures were tested, namely, Vinsol-I and Vinsol-II. Another experimental variable in the present study corresponded to the water reducing admixture types. Both water reducing admixtures (WRA) as well as high range water reducing admixtures (HRWA) or superplasticizers were investigated. Research with WRA, here designated as series-I tests, included brands B and D, whereas, research with HRWA is termed as series II tests, involved brands A, B, C, and D. Series I tests included four sets of concrete mixtures, and series II tests involved thirteen mixtures. In each series, the mixture proportions were kept constant, except for the air-entraining agents. In series II tests, additional mixtures were prepared with higher dosages of the air-entraining admixtures. This was done for brand-D based on the manufacturer's recommendations. These mixtures pertain to samples SVD2 through SVD3 in Table 7.

## Materials and Mix Proportions

Constituents of the concretes produced for series I, and II tests are given below. Note the differences in the water reducing admixtures for series I, and II. All the materials selected conform to ASTM requirements, and they include:

- **Cement:** Saylor's Type I Portland cement conforming to ASTM C 150.
- **Coarse Aggregate:** the ¾ inch crushed gravel, conforming to ASTM C 33 gradation requirement, was employed as the coarse aggregate. The particle size distribution of coarse aggregates is presented in table 2.
- **Fine Aggregate:** ASTM No. 2 river sand. Grading data is also given in table 3.
- **Water Reducing Agent for Series-I:** Master Builder's Pozzolith 122-N, a **WRA** with dosage of 8 fluid oz per 100 lb. cement. Meeting the ASTM designation C 494 as a type A and F mixture, C1017 as Type I admixture.
- **Water Reducing Agent for Series-II:** Daracem 19 (Producer: Grace Co.), a **HRWA** with dosage of 8 fluid oz per 100 lb. cement. Meeting the ASTM designation C 494 as a type A and F mixture, C1017 as Type I admixture.
- **Air-entraining admixtures:** all meet the ASTM designation C233 standard specification for air-entraining admixtures for concrete. The mix proportion and specimen designation according to air-entraining admixtures are given in tables 4 and 5.

## Materials samples designation

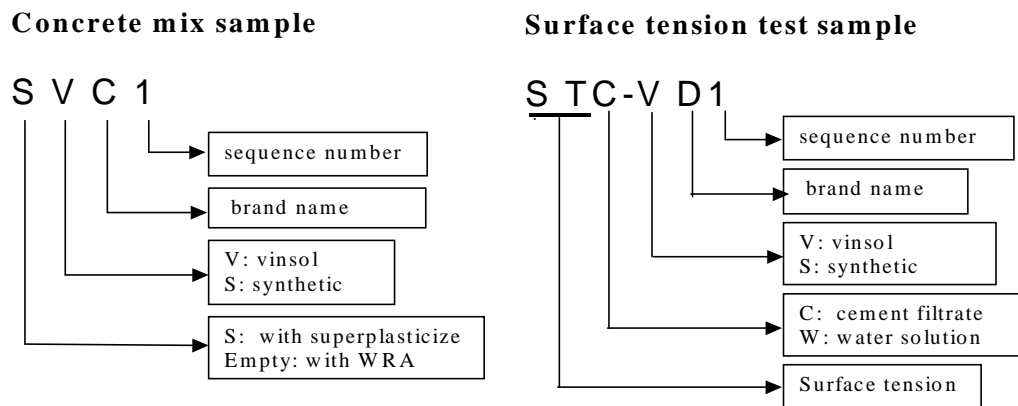


Figure S1. materials samples designation

Table 2. Coarse aggregate sieve analysis (22 lb. sample)

	Retained Weight percent	Cumulative weight passing	Passing Weight percent	Specification weight percent passing

2 in	0	10	100	100
1.5 in	0	10	100	100
¾ in	9.6	9.04	90.4	90 -100
3/8 in	84.6	1.54	15.4	20 -55
No.4	98.2	0.18	1.8	0 -10
Total	192.4	30.76	307.6	

Table 3. Fine aggregate sieve analysis (1.1 lb. sample)

	Retained Weight percent	Cumulative weight passing	Passing Weight percent	Specification weight percent passing
No.4	4	0.48	96	95 -100
No.8	16	0.42	84	80 -100
No.16	32	90.32	68	50 - 85
No.30	48	0.26	52	25 - 60
No.50	76	0.12	24	10 -30
No.100	96	0.02	4	2 -10
Total	276	1.64	328	

Table 4. Concrete mix design (Series-I)

Material	Quantity per cubic yard
Cement	720 lb.
Water	295 lb.
Coarse aggregate	1820 lb.
Fine aggregate	1151 lb.
WRA (MB Pozzoloth 122-N) (8 oz per 100 lb. cement)	57.6 oz
Water-cement ratio	0.41
Air-entraining admixture	Varied (see Table 6)

Table 5. Concrete mix design (Series-II)

Material	Quantity per cubic yard
Cement	720 lb.
Water	288 lb.

Coarse aggregate	1820 lb.
Fine aggregate	1151 lb.
HWRA DARACEM 19 (8 oz per 100 lb. cement)	57.6 oz
Water-cement ratio	0.40
Air-entraining admixture	Varied (see Table 7)

Table 6. Concrete mix designation according to air-entraining admixtures (Series-I)

Concrete mix designation	Air-entraining admixture brand	Type	Number of specimens	Dosage (oz/100 lb. cement)
VB	Brand-B	Vinsol	8	1.0
SB	Brand-B	Synthetic	8	1.0
VD1	Brand-D	Vinsol	8	1.0
SD1	Brand-D	Synthetic	8	1.0

Table 7. Concrete mix designation according to air-entraining admixtures (Series-II)

Concrete mix designation	Number of specimen	Air-entraining admixture brand	Type	Dosage (oz/100 lb. cement)
SVA	15	Brand-A	Vinsol	1.0
SSA	15	Brand-A	Synthetic	1.0
SVB	15	Brand-B	Vinsol	1.0
SSB	15	Brand-B	Synthetic	1.0
SVC1	15	Brand-C	Vinsol-I	1.0
SVC2	15	Brand-C	Vinsol-II	1.0
SSC	15	Brand-C	Synthetic	1.0
SVD1	15	Brand-D	Vinsol	1.0
SSD1	15	Brand-D	synthetic	1.0
SVD2	15	Brand-D	Vinsol	2.0
SSD2	15	Brand-D	synthetic	2.0
SVD3	15	Brand-D	Vinsol	4.0
SSD3	15	Brand-D	synthetic	4.0

### Mix Procedures and Compressive Strength Tests

Concrete mixtures were prepared in a drum-type mixer. Constituents were added in the sequence starting with the coarse aggregate, then cement and sand. Air-entraining agents were premixed with water and added directly to the sand before the addition of the water reducing agent. The total mixing time was 4.5 minutes. The air content in fresh state was measured according to ASTM C231-91b by the pressure method (Type A meter) and C138-83 (gravimetric method). Specimens were cast in disposable 4 × 8 inch plastic cylindrical molds. Freshly cast specimens were kept in the mold for 24 hours, and then they were demolded and stored in a moist-cure room. At one day prior to testing, they were taken out of curing room and their ends were capped for uniaxial compression tests.

The MTS materials testing system and associated TestStar™ IIs controller 793.00 was employed for the determination of compressive strengths of the concrete samples according to ASTM C39-86 (Figure 8). The maximum load capacity of the MTS is 150 kips. The load was applied under displacement control at a rate of 0.0001 inch per second.



Figure 8. MTS Materials testing system

### **Air Void Analysis**

Automated linear traverse method with the image processing system was employed for the analysis of the air void parameters in the hardened state as per ASTM C 457. This system was described in Phase I report, and for completeness it will be further described in the appendix section of this report (Appendix-A). Concrete cylinders were sliced, polished and surface-handled for proper characterization of the air void system as per ASTM C 457. For each cylinder, three slices were analyzed for a total traverse length of 104 inch and a total coverage area of 12.48 square inch. This traverse length was based on the maximum aggregate size as per ASTM C 457 standard. The measured parameters include air content, specific surface, spacing factor, paste air ratio, void frequency and average chord length. The concrete slice preparation sequence, procedures and instrumentation for air void analysis are presented in figures 9 and 10.

In general, to ensure adequate frost protection, the smaller the spacing factor, the more durable the concrete (Fig.3). The voids should be small, in the range 0.05 to 1.25 mm (0.002 inch to 0.05 inch) diameter to ensure that the required spacing factor is obtained at relatively low air contents. The resolution or the smallest air void size discernable by the present system is 8 micrometer (0.008 mm). Air void parameters for series-I tests were measured in two different ways. Group-I measurements included only the smaller range void sizes pertaining to the range 0.008 to 1.25 millimeter entrained air void system. Group-II

measurements on the same slices encompassed measurement of all the entrained air void sizes (including those larger than 1.25 mm). Assuming that the Entrapped air voids are not spherical in shape, they were automatically excluded as the system only measures spherical voids. Air void distribution, and data pertaining to the various parameters of the air void systems for both measurements (Groups I and II) are provided in this report. Series II tests (HRWA) were performed considering the bubble sizes in the range 0.008 mm to 1.25-mm.





Figure 9. Concrete slice sample preparation. (From left to right: lapping machine, slice after polishing, painting materials, sample ready for test)



Figure 10. Automated linear traverse system

## Surface Tension Measurements

Surface tension measurements involved experimentation with two types of solutions: (1) admixtures dissolved in water; and (2) filtrates of cement paste containing the admixtures. In all the samples, the mix ratio of air-entraining agent to water was such that the dosage of 1.0 oz per 100 lbs. of cement corresponded to 1.0 oz per 40 lbs. of water. In the case of cement filtrates, the paste consisted of 20-gram of type I cement per 1230-ml of the solution consisting of the water and the air-entraining agent. The dosage of air entraining agent was selected based on the recommended values of the manufactures, which were detailed along with other parameters in tables 8 and 9.

Measurements were conducted on a computer controlled and video-based optical contact angle device. The technique involved image analysis and profile optimization of the admixture solution droplets. The solution was initially dosed to a needle tip with a diameter of 3.05mm to form an elongated pendant drop using an electrical syringe with dosing rate of 5- $\mu$ L/s and volume of 35- $\mu$ L, which was controlled through algorithms controlled by a computer. The average of three measurements was considered for each sample. A measurement accuracy of 0.01 dyne/cm was achieved in the measurements with this device. Details corresponding to the surface tension measurement methodologies and instrumentation are given in appendix section of this report (Appendix-B). All the tests were conducted with the collaboration of Motorola Advanced Technology Center (MATC) in Illinois, and the Future Digital Scientific in New York.

Table 8 . Surface tension sample designations, dosages, and densities (water solution)

Sample	Air-entraining admixture brand	Applied dosage (fl oz/100 lb. cement)	Density (gm/cm <sup>3</sup> )
STW-VA	Brand-A	1.0	0.9946
STW-SA	Brand-A	1.0	0.9940
STW-VB	Brand-B	1.0	0.9984
STW-SB	Brand-B	1.0	0.9984
STW-VC1	Brand-C	1.0	0.9984
STW-VC2	Brand-C	1.0	0.9983
STW-SC	Brand-C	1.0	0.9981
STW-VD1	Brand-D	1.0	0.9985
STW-SD1	Brand-D	1.0	0.9985
STW-VD2	Brand-D	2.0	0.9985
STW-SD2	Brand-D	2.0	0.9985
STW-VD3	Brand-D	4.0	0.9985
STW-SD3	Brand-D	4.0	0.9985

Table 9. Surface tension sample designations, dosages, and densities (filtrate of cement paste)

Sample	Source	Applied dosage (fl oz/100 lb. cement)	Density (gm/cm <sup>3</sup> )
STC-VA	Brand-A	1.0	0.9986
STC-SA	Brand-A	1.0	0.9985
STC-VB	Brand-B	1.0	0.9985
STC-SB	Brand-B	1.0	0.9985
STC-VC1	Brand-C	1.0	0.9985
STC-VC2	Brand-C	1.0	0.9986
STC-SC	Brand-C	1.0	0.9986
STC-VD1	Brand-D	1.0	0.9986
STC-SD1	Brand-D	1.0	0.9986
STC-VD2	Brand-D	2.0	0.9986
STC-SD2	Brand-D	2.0	0.9986
STC-VD3	Brand-D	4.0	0.9986
STC-SD3	Brand-D	4.0	0.9986

## EXPERIMENTAL RESULTS

### Series-I (WRA)

Compression test results as well as air contents in fresh and hardened states are given in table 10 for groups-I and II, respectively. The automated image analysis system was employed for the determination of air bubble parameters in hardened state based on the linear traverse methodology. The linear traverse procedure was repeated three times for each sample to assure repeatability. Appendix-A details the reliability analysis and comparison of the manual and the automated linear traverse methods. As stated previously, groups I and II measurements pertain to the same concrete and slices, they only differ for the upper bound measurement limits on the bubble sizes placed on the linear traverse system. It is impossible to follow the same traverse path for the two measurements (groups I and II), and therefore, there will be differences in bubble count measurements at smaller bubble size levels as well. As shown in these tables the compressive strength results are based on three replicate tests. The air void parameters for groups-I and II, as computed from the data in hardened state, are given in tables 11 and 12, respectively. Tables 13 and 14 compare the bubble sizes and their distribution for the Vinsol and Synthetic agents for brands B and D, respectively (group-I). Similarly, Tables 15 and 16 compare the bubble sizes and their distribution for the Vinsol and Synthetic agents for brands B and D, based on group-II bubble size measurement criteria.

Table 10. Compressive strength and air content for series-I experiments (Groups I and II)

Sample	Slump (inch)	Maximum load1 (kips)	Maximum load2 (kips)	Maximum load3 (kips)	Average load (kips)	$f'_{c1}$ (ksi)	$f'_{c2}$ (ksi)	$f'_{c3}$ (ksi)	$\overline{f'_c}$ (ksi)	Air content (pressure)	Group-I Air content in hardened concrete (%)	Group-II Air content in hardened concrete (%)
VB	3.75	77.78	77.59	78.02	77.80	6.19	6.18	6.21	<b>6.19</b>	6.0	5.3167	6.10
SB	4.00	78.22	76.65	76.53	77.13	6.23	6.10	6.09	<b>6.14</b>	5.6	5.3849	6.42
VD1	3.50	80.05	81.39	—	80.72	6.37	6.48	—	<b>6.43</b>	4.5	4.0177	4.95
SD1	5.00	74.14	71.27	73.92	73.11	5.90	5.67	5.89	<b>5.82</b>	6.2	5.4387	6.38

Table 11. Parameters of measured air-void system in hardened state (Series-I, Group-I)

sample	Air-entraining agents type: V-vinsol S-synthetic	Average chord length (mm)	Paste-air ratio	Air content (%)	Spacing factor (mm)	Specific surface (mm <sup>2</sup> /mm <sup>3</sup> )	Void frequency (No. per mm)
VB	V	0.1739	5.1159	5.3167	0.2035	23.0021	0.3057
SB	S	0.1652	5.0511	5.3849	0.1922	24.2174	0.3260
VD1	V	0.1631	6.7700	4.0177	0.2168	24.5307	0.2464
SD1	S	0.1936	5.0012	5.4387	0.2242	20.6630	0.2809

Table 12. Parameters of air-void system in hardened state (Series-I, Group-II)

sample	Air-entraining agents type: V-vinsol S-synthetic	Average chord length (mm)	Paste-air ratio	Air content (%)	Spacing factor (mm)	Specific surface (mm <sup>2</sup> /mm <sup>3</sup> )	Void frequency (No. per mm)
VB	V	0.1832	4.4616	6.0965	0.2014	21.8545	0.3125
SB	S	0.1799	4.2367	6.4201	0.1906	22.2316	0.3500
VD1	V	0.1743	5.4941	4.9507	0.2108	22.9425	0.2640
SD1	S	0.2056	4.2635	6.3798	0.2192	19.4518	0.2903

Table 13. Comparison of air void distribution for VB and SB (Series-I Group-I)

Diameter of air void In micrometer*	Number of air voids per 104 inch traverse length	
	VB: Vinsol Resin	SB: Synthetic type
20	22	12
40	71	65
60	61	67
80	118	135
100	48	77
120	80	98
140	43	52
160	66	62
180	33	34
200	35	31
250	50	65
300	48	49
350	31	38
400	40	23
500	33	29
600	19	15
800	15	14
1000	1	2
Total	814	868
Air content(%)	5.3167	5.3849
Specific Surface (mm <sup>-1</sup> )	23.0021	24.2174
Spacing factor (mm)	0.2035	0.1922
Paste-air ratio	5.1159	5.0511
Paste content (%)	27.2	27.2
Average Chord length (mm)	0.1739	0.1652
Void frequency (No. per mm)	0.3057	0.3260

\* These figures provide upper limits of diameter intervals: for example, 80 pertain to the size of air voids whose size fall into the range between 60 and 80 microns.

Table 14. Comparison of air void distribution for VD1 and SD1 (Series-I Group-I)

Diameter of air void In micrometer*	Number of air voids per 104 inch traverse length	
	VD1: Vinsol Resin	SD1: Synthetic type
20	5	20
40	56	52
60	53	46
80	96	85
100	57	58
120	64	75
140	44	34
160	40	53
180	28	21
200	36	37
250	39	59
300	41	51
350	36	40
400	20	32
500	23	49
600	15	15
800	3	17
1000		4
Total	656	748
Air content(%)	4.0177	5.4387
Specific Surface (mm <sup>-1</sup> )	24.5307	20.6630
Spacing factor (mm)	0.2168	0.2242
Paste-air ratio	6.7700	5.0012
Paste content (%)	27.2	27.2
Average Chord length (mm)	0.1631	0.1936
Void frequency (No. per mm)	0.2464	0.2809

\* These figures provide upper limits of diameter intervals: for example, 80 pertain to the size of air voids whose size fall into the range between 60 and 80.

Table 15 Comparison of air void distribution for VB and SB (Series-I Group-II)

Diameter of air void In micrometer*	Number of air voids per 104.8 inch traverse length	
	VB: Vinsol Resin	SB: Synthetic type
20	16	17
40	64	62
60	70	72
80	104	137
100	60	88
120	72	104
140	50	50
160	69	70
180	32	27
200	45	47
250	74	66
300	33	38
350	30	48
400	28	39
500	42	28
600	16	21
800	19	13
1000	1	1
>1000	7	4
Total	832	932
Air content(%)	6.0965	6.4201
Specific Surface ( $\text{mm}^{-1}$ )	21.8545	22.2316
Spacing factor (mm)	0.2014	0.1906
Paste-air ratio	4.4616	4.2367
Paste content (%)	27.2	27.2
Average Chord length (mm)	0.1832	0.1799
Void frequency (No. per mm)	0.3125	0.3500

\* The figure give upper limits of diameter intervals: for example, 80 pertains to the size of air voids whose size fall into the range between 60 and 80.



Table 16. Comparison of air void distribution for VD1 and SD1 (Series-I Group-II)

Diameter of air void In micrometer*	Number of air voids per 104.8 inch traverse length	
	VD1: Vinsol Resin	SD1: Synthetic type
20	9	10
40	58	61
60	52	45
80	100	81
100	61	59
120	67	76
140	38	36
160	56	47
180	25	36
200	41	33
250	60	74
300	35	49
350	26	39
400	21	29
500	27	42
600	9	14
800	7	16
1000	4	10
>1000	7	16
Total	703	773
Air content(%)	4.9507	6.3798
Specific Surface (mm <sup>-1</sup> )	22.9425	19.4518
Spacing factor (mm)	0.2108	0.2192
Paste-air ratio	5.4941	4.2635
Paste content (%)	27.2	27.2
Average Chord length (mm)	0.1743	0.2056
Void frequency (No. per mm)	0.2640	0.2903

\* The figure give upper limits of diameter intervals: for example, 80 pertains to the size of air voids whose size fall into the range between 60 and 80.

**Series-II (HRWA)**

Series II tests involved the use of high range water reducers in the mixtures for brands A, B, C, and D. Compression test results as well as air contents in fresh and hardened states are given in table 17. Both gravimetric as well as pressure methods were used for the determination of air content in fresh state. The air void parameters in the hardened state are given in table 18. Tables 19 through 22 correspond to the comparison of air void size distributions for the Vinsol and Synthetic resins. Each table represents comparison of the resins from the same manufacturers.

### **Series-II at Higher Dosages of Air Entraining Admixtures**

Results described thus far pertains to experimental analysis of mixtures prepared based on the recommended dosage of 1.0 oz per 100-pound of cement by the manufacturers of the admixtures. In addition to the normal dosage of 1-oz, the manufacturers of brand-D had also recommended higher dosages of their synthetic and Vinsol resin admixtures in proportioning of concrete mixtures. Accordingly, four additional groups of mixtures were prepared comprising of 2 and 4 fluid ounces of synthetic and Vinsol resin admixtures. Table 23 corresponds to the specimen designations, compressive strengths and the air contents as measured by the gravimetric and pressure methods for specimens produced through addition of brand-D admixtures at these higher dosages. Tables 24 and 25 detail the air bubble size distribution data and air void parameters at hardened state as analyzed through the image analysis system. Air void parameters at the hardened state for all the samples at higher dosages of air entraining admixtures are given in table 26.

### **Surface Tension Test Results**

Results from the measurement of surface tension of the air entraining admixtures in water as well as in cement filtrates are given in table 27. These results represent the average of three replicate tests per sample with a standard deviation of less than 0.2 dyne/cm. Surface tension data for samples containing higher dosages of admixtures (brand D) are given in table 28. Again, table 28 contains data for the admixture in water as well as in cement filtrate. Analysis of data will be discussed next.

Table 17. Compressive strength and air content for series II specimens

sample	Maximum load1 (kips)	Maximum load2 (kips)	Maximum load3 (kips)	Average load (kips)	$f'_{c1}$ (ksi)	$f'_{c2}$ (ksi)	$f'_{c3}$ (ksi)	$\overline{f'_c}$ (ksi)	Air content (gravimetric)	Air content (pressure)	Air content in hardened concrete (%)
SVA	84.56	81.50	76.54	80.87	6.73	6.49	6.09	6.44	6.03	5.44	4.7575
SSA	72.22	70.70	69.16	70.70	5.75	5.63	5.50	5.63	7.12	6.84	6.1218
SVB	80.72	86.96	83.25	83.64	6.42	6.92	6.62	6.66	6.87	6.56	6.2043
SSB	83.35	80.27	85.17	82.93	6.63	6.39	6.78	6.60	7.02	6.67	6.3636
SVC1	84.01	82.89	80.42	82.44	6.69	6.60	6.40	6.56	6.39	6.05	5.6100
SVC2	90.56	81.90	85.50	85.99	7.21	6.52	6.80	6.84	5.62	5.01	4.4447
SSC	85.88	77.31	68.32	77.17	6.83	6.15	5.44	6.14	6.00	5.89	5.3029
SVD1	78.11	76.50	79.29	77.97	6.22	6.09	6.31	6.20	5.74	5.68	5.3344
SSD1	73.48	73.44	72.87	73.26	5.85	5.84	5.80	5.83	7.91	7.80	7.5556

Table 18. Parameters of air-void system in hardened state for series II specimens

sample	Air-entraining agents type: V-vinsol S-synthetic	Average chord length (mm)	Paste-air ratio	Air content (%)	Spacing factor (mm)	Specific surface (mm <sup>2</sup> /mm <sup>3</sup> )	Void frequency (No. per mm)
SVA	V	0.2172	5.7172	4.7575	0.2674	18.4147	0.2190
SSA	S	0.2652	4.4431	6.1218	0.2910	15.0809	0.2308
SVB	V	0.2447	4.3841	6.2043	0.2668	16.3455	0.2535
SSB	S	0.2046	4.2743	6.3636	0.2187	19.5486	0.3110
SVC1	V	0.2052	4.8455	5.6100	0.2343	19.4965	0.2734
SVC2	V	0.1943	6.1196	4.4447	0.2468	20.5855	0.2287
SSC	S	0.2664	5.1292	5.3029	0.3121	15.0158	0.1991
SVD1	V	0.1999	5.0989	5.3344	0.2336	20.0107	0.2669
SSD1	S	0.2722	3.6000	7.5556	0.2450	14.6948	0.2776

Table 19. Comparison of air void distribution for SVA and SSA (Series II)

Diameter of air void In micrometer*	Number of air voids per 208 inch traverse length	
	Vinsol Resin	Synthetic type
20	15	13
40	91	70
60	111	72
80	162	140
100	96	87
120	85	118
140	53	67
160	71	84
180	38	47
200	52	65
250	45	104
300	45	64
350	36	51
400	39	51
500	37	52
600	43	35
800	39	38
1000	17	23
>1000	38	48
Total	1113	1229
Air content(%)	4.7575	6.1218
Specific Surface ( $\text{mm}^{-1}$ )	18.4147	15.0809
Spacing factor (mm)	0.2674	0.2910
Paste-air ratio	5.7172	4.4431
Paste content (%)	27.2	27.2
Average Chord length (mm)	0.2172	0.2652
Void frequency (No. per mm)	0.2190	0.2308

\* The figure give upper limits of diameter intervals: for example, 80 pertains to the size of air voids whose size fall into the range between 60 and 80.

Table 20. Comparison of air void distribution for SVB and SSB (Series II)

Diameter of air void In micrometer*	Number of air voids per 208 inch traverse length	
	Vinsol Resin	Synthetic type
20	21	20
40	72	126
60	84	125
80	158	194
100	94	107
120	126	178
140	61	69
160	90	107
180	43	56
200	65	80
250	108	131
300	68	74
350	66	88
400	73	74
500	69	70
600	51	63
800	55	48
1000	25	6
>1000	20	22
Total	1349	1638
Air content(%)	6.2043	6.3636
Specific Surface ( $\text{mm}^{-1}$ )	16.3455	19.5486
Spacing factor (mm)	0.2668	0.2187
Paste-air ratio	0.3841	4.2743
Paste content (%)	27.2	27.2
Average Chord length (mm)	0.2447	0.2046
Void frequency (No. per mm)	0.2535	0.3110

\* The figure give upper limits of diameter intervals: for example, 80 pertains to the size of air voids whose size fall into the range between 60 and 80.

Table 21. Comparison of air void distribution for SVC1, SVC2 and SSC (Series II)

Diameter of air void In micrometer*	Number of air voids per 208 inch traverse length		
	Vinsol-I	Vinsol-II	synthetic
20	17	18	10
40	103	89	69
60	153	135	74
80	227	214	118
100	87	92	77
120	121	122	78
140	80	75	52
160	118	66	58
180	49	50	26
200	57	34	65
250	98	72	80
300	64	61	61
350	48	32	54
400	42	33	39
500	70	36	41
600	34	18	38
800	39	30	61
1000	28	25	29
>1000	21	20	45
Total	1456	1222	1075
Air content(%)	5.6100	4.4447	5.3029
Specific Surface ( $\text{mm}^{-1}$ )	19.4965	20.5855	15.0158
Spacing factor (mm)	0.2343	0.2468	0.3121
Paste-air ratio	4.8455	6.1196	5.1292
Paste content (%)	27.2	27.2	27.2
Average Chord length (mm)	0.2052	0.1943	0.2664
Void frequency (No. per mm)	0.2734	0.2287	0.1991

\* The figure give upper limits of diameter intervals: for example, 80 pertains to the size of air voids whose size fall into the range between 60 and 80.

Table 22. Comparison of air void distribution for SVD1 and SSD1 (Series II)

Diameter of air void In micrometer*	Number of air voids per 208 inch traverse length	
	Vinsol Resin	Synthetic type
20	28	18
40	98	66
60	109	86
80	202	148
100	126	104
120	128	136
140	77	84
160	88	127
180	52	67
200	56	73
250	114	134
300	74	71
350	63	71
400	54	61
500	46	70
600	42	53
800	40	43
1000	8	23
>1000	19	43
Total	1424	1478
Air content(%)	5.3344	7.5556
Specific Surface ( $\text{mm}^{-1}$ )	20.0107	14.6948
Spacing factor (mm)	0.2336	0.2450
Paste-air ratio	5.0989	3.6000
Paste content (%)	27.2	27.2
Average Chord length (mm)	0.1999	0.2722
Void frequency (No. per mm)	0.2669	0.2776

\* The figure give upper limits of diameter intervals: for example, 80 pertains to the size of air voids whose size fall into the range between 60 and 80.



Table 23. Specimen designations, compressive strengths and the air contents for samples produced through additional dosages of brand-D admixtures

sample	Air-entraining agents type: V-vinsol S-synthetic	Admixture dosage (fl oz/100lb cement)	Maximum load1 (kips)	Maximum load2 (kips)	Maximum load3 (kips)	Average load (kips)	$f'_{c1}$ (ksi)	$f'_{c2}$ (ksi)	$f'_{c3}$ (ksi)	$\overline{f'_c}$ (ksi)	Air content (gravimetric)	Air content (pressure)
SVD1	V	1.0	78.11	76.50	79.29	77.97	6.22	6.09	6.31	6.20	5.74	5.68
SSD1	S	1.0	73.48	73.44	72.87	73.26	5.85	5.84	5.80	5.83	7.91	7.80
SVD2	V	2.0	76.17	70.86	71.11	72.71	6.06	5.64	5.66	5.78	6.50	6.21
SSD2	S	2.0	76.51	76.35	79.96	77.61	6.09	6.08	6.36	6.18	5.07	4.95
SVD3	V	4.0	70.22	68.04	71.42	69.88	5.59	5.41	5.68	5.56	6.86	6.77
SSD3	S	4.0	75.65	72.81	70.09	72.85	6.02	5.79	5.58	5.80	5.61	5.20

Table 24. Comparison of air void distribution for SVD2 and SSD2

Diameter of air void In micrometer* <sup>1</sup>	Number of air voids per 208 inch traverse length	
	Vinsol Resin	Synthetic type* <sup>2</sup>
20	13	15
40	67	76
60	87	105
80	124	132
100	89	91
120	128	115
140	49	44
160	84	69
180	40	34
200	55	53
250	117	63
300	68	48
350	60	47
400	53	38
500	68	41
600	45	26
800	47	9
1000	14	8
>1000	34	10
Total	1242	1024
Air content(%)	5.8308	4.5237
Specific Surface (mm <sup>-1</sup> )	16.0010	21.4630
Spacing factor (mm)	0.2804	0.2348
Paste-air ratio	4.6649	6.0127
Paste content (%)	27.2	27.2
Average Chord length (mm)	0.2500	0.1864
Void frequency (No. per mm)	0.2332	0.2427

\*1 The figure give upper limits of diameter intervals: for example, 80 pertains to the size of air voids whose size fall into the range between 60 and 80.

\*2 The traverse length is 166.4 inch.

Table 25. Comparison of air void distribution for SVD3 and SSD3

Diameter of air void In micrometer*	Number of air voids per 208 inch traverse length	
	Vinsol Resin	Synthetic type
20	14	16
40	54	62
60	60	68
80	115	121
100	92	83
120	106	98
140	65	66
160	68	89
180	40	49
200	83	54
250	117	76
300	95	63
350	71	49
400	61	47
500	84	57
600	51	37
800	58	32
1000	18	9
>1000	31	17
Total	1283	1093
Air content (%)	6.4325	4.6151
Specific Surface ( $\text{mm}^{-1}$ )	14.9831	17.7909
Spacing factor (mm)	0.2822	0.2807
Paste-air ratio	4.2285	5.8937
Paste content (%)	27.2	27.2
Average Chord length (mm)	0.2670	0.2248
Void frequency (No. per mm)	0.2409	0.2053

\* The figure give upper limits of diameter intervals: for example, 80 pertains to the size of air voids whose size fall into the range between 60 and 80.

Table 26 Parameters for measured air-void system of samples with additional dosage for Brand-D admixtures

Sample	Air-entraining agents type: V-vinsol S-synthetic	Average chord length (mm)	Paste-air ratio	Air content (%)	Spacing factor (mm)	Specific surface (mm <sup>-1</sup> )	Void frequency (No. per mm)
SVD1	V	0.1999	5.0989	5.3344	0.2336	20.0107	0.2669
SSD1	S	0.2722	3.6000	7.5556	0.2450	14.6948	0.2776
SVD2	V	0.2500	4.6649	5.8308	0.2804	16.0010	0.2332
SSD2	S	0.1864	6.0127	4.5237	0.2348	21.4630	0.2427
SVD3	V	0.2670	4.2285	6.4325	0.2822	14.9831	0.2409
SSD3	S	0.2248	5.8937	4.6151	0.2807	17.7909	0.2053

Table 27. Surface tension measurement result (dyne/cm)

Sample	STW-VA	STW-SA	STW-VB	STW-SB	STW-VC1	STW-VC2	STW-SC	STW-VD1	STW-SD1
Surface tension (dyne/cm)	59.29	56.69	55.96	48.92	59.4	63.4	40.5	61.22	51.44
sample	STC-VA	STC-SA	STC-VB	STC-SB	STC-VC1	STC-VC2	STC-SC	STC-VD1	STC-SD1
Surface tension (dyne/cm)	52.95	51.36	58.33	60.37	47.11	57.52	52.98	60.15	58.17

Table 28. Surface tension of solutions with Brand-D admixtures at higher dosages of air entraining admixtures

Sample	STW-VD1	STW-SD1	STW-VD2	STW-SD2	STW-VD3	STW-SD3
Surface tension (dyne/cm)	61.22	51.44	52.02	57.46	49.23	49.54
sample	STC-VD1	STC-SD1	STC-VD2	STC-SD2	STC-VD3	STC-SD3
Surface tension (dyne/cm)	60.15	58.17	54.50	58.74	50.32	53.90

## ANALYSIS OF RESULTS

### Series-I (WRA)

It is important to provide some insight into the differences between air content measurements in fresh and hardened concretes. The automated linear traverse system was programmed to detect bubble sizes ranging from 8 micron (resolution of the system) to 1.25 mm (Group-I measurements). In general, while large bubbles are not considered to be entrained, there are no set standards as to what is considered large. Also, the pressure meter does not discriminate between entrapped and entrained air and for this reason, pressure meter measured air contents are consistently higher than the linear traverse results reported for series-I, group I or series-II tests (Table 10-Group-I and Table 17). On the other hand, some studies suggest that the pressure meter is not capable of measuring the air content of the extremely small bubbles. It is however, understood that the larger air bubbles produce more of the air content by volume. Accordingly, larger pressure meter readings suggest existence of larger than 1.25mm bubbles in the concrete samples under study. To examine existence and effect of larger bubbles, the program routine for the automated linear traverse method was altered to include all the spherical voids that are larger than 1.25 mm. Series-I measurements were repeated and the new measurements are provided under group-II measurements (table 12).

A more convenient approach in comparing the air void distribution in the air-entrained concretes is through bar charts. For this reason, bar chart version of tables 13 through 16 is provided in Figs 11 through 14. Comparison of brand B data (Figs 11 and 12) indicates that except for the very small bubble sizes of 60 microns or less in diameter, the Synthetic agent produced more of the air bubbles including those in the size ranges of small to medium. Interestingly, examination of group-II measurements in Fig 12 indicated that the Vinsol admixture produced slightly more of the very large bubbles. The very large bubbles are considered bubbles larger than 1-mm. However, all the bubbles were smaller than 2-mm. Quantitatively, these results are explainable by the smaller spacing factors and larger specific surfaces for SB when compared with VB (tables 11 and 12). The air void systems for VB and SB are further compared in Figs 15 and 16. Comparison of the pressure meter readings for VB and SB showed lower air content for SB, but the linear traverse results both in group-I and II measurement categories indicated higher air contents for SB. Nevertheless, data including the air void characteristics, i.e. spacing factor, indicates that the pressure meter readings for SB were on the low side. The difference in strength for the two concrete types was statistically minimal with an average decrease of 50 Psi in compressive strength for SB. The effect of Synthetic air entraining agent on the air void characteristics and the compressive strength of concrete was more pronounced for Brand-D admixtures. For both VD1 and SD1, the pressure meter readings were more in line with the

linear traverse results (table 10). Moreover, the synthetic agent (SD1) produced much higher total air than the Vinsol resin agent (VD1) with the differences in total air contents of about 1.7% and 1.4% by the pressure and the linear traverse methods respectively. In compare to VD1, a 9.5% decrease in strength was observed for SD1. As shown in tables 11 and 12, in terms of the spacing factor and specific surface both VD1 and SD1 performed poorly, with SD1 producing more of the larger bubbles (Figs 13-14). Magnified air bubble images for VD1 and SD1 are shown in Figs 17 and 18.

An interesting result pertains to the concretes produced by the two different brand synthetic agents (SB and SD1). The compressive strength of SB was 5.2% larger than SD1, and as shown in table 10, for all practical purposes the air contents of the two synthetic agents SB (brand B) and SD1 (brand D) as measured by the linear traverse method are the same (about 6.4%). Fig. 19 compares the air void distribution of SB and SD1. As it is shown, SB produces more of the smaller size bubbles, and conversely, SD1 produces more of the air bubbles of 200 micron in diameter and more. For these samples (SB and SD1), the total number of bubbles for the length of traverse can be obtained from tables 15 and 16. SB possessed higher compressive strength and produced 159 more air bubbles than SD1 at the same level of total air content. These results suggest the larger bubble sizes as the primary cause for the lower strength in SD1.

General findings pertaining to the analysis of results based on series-I tests are summarized below:

1. For both brands (B and D), synthetic air-entraining admixtures created more air bubbles than their Vinsol resin counterparts (Tables 13-16).
2. More air bubbles do not necessarily result in lower strengths. The reduction in strength at the same level of total air is associated with the production of larger bubble sizes (SB and SD1).
3. For both brands (B and D), concretes produced with synthetic air entraining admixtures possessed lower strengths (Table 10). However, the reduction in strength for brand B was minimal (0.8%). In fact, in terms of air void characteristics, Brand B synthetic agent produced a more durable concrete than the concrete produced by the Vinsol resin admixture.
4. The extent which synthetic air entraining agents affect the air void characteristics and therefore the compressive strength are brand sensitive (tables 11-12). Depending on the brand, Synthetic agents influence the air void system in two ways. Some increase the total number of air bubbles; others increase the number of very large bubbles; and the third category does both.

## **Series-II (HRWA)**

The experimental program involved proportioning of admixtures at the normal recommended dosage of 1.0 Oz per 100 pounds of cement as per manufacturer recommendations (SVA through SSD1). Additional experiments were performed on the brand-D admixtures at higher dosages (SVD2 through SSD3). The higher dosage experiments were conducted in order to provide preliminary information for recommendation to NJDOT and future direction of research. Comparison of results will be performed in this section for mixtures SVA through SSD1. Results from experimentation with SVD2 through SSD3 will be discussed in the section entitled higher dosage mixtures.

Figs 20 through 23 represent the air void size distribution through bar chart representations of tables 19 through 22. These results together with data pertaining to the compressive strength, air content, and air void parameters in tables 17 and 18 are employed for the analysis of the results. Since series-I (WRA) tests involved brands B and D, it is appropriate to start the analysis of series-II data with brands B and D. As shown in table 17, the compressive strengths and air contents of SVB and SSB (brand B) are comparable with a 0.1% and 2% differences for the compressive strength and air content respectively. In a manner similar to the results obtained for series-I tests, brand B synthetic agent (SSB) produced better air void distribution as shown in Fig. 21, and demonstrated by the spacing factor and specific surfaces. On the other hand comparison of SVD1 and SSD1 reveal 6% strength loss for SSD1 in compare to SVD1 at a more than 2% by volume difference in total air content. As shown in Fig.23 and demonstrated by the spacing factors and the specific surfaces, SSD1 produced larger bubbles, and therefore, smaller specific surface at a larger spacing factor. Magnified images of the air bubble distribution within the above-mentioned samples are shown in Figs 24 and 25.

These results are commensurate with the results obtained for brands B and D in series-I experiments, except for the fact that the HRWA samples produced more air bubbles. As shown by the previous research (Mather, 1979) and reinforced by the present study results, the addition of high range water reducers to air entrained concrete increase the spacing factor and decrease the specific surface area of the air void system. However, present study's results suggest that the effects of synthetic agents on the air void system are independent of the effects of high range water reducers. Brands B and D in series-I and series-II experiments both reacted similarly to the different admixture types. High range water reducers superimpose additional voids. Moreover, these effects are brand sensitive as the synthetic agents in brands B and D produced concretes with contrasting air void characteristics. The effect of each admixture brand on the air void system should be considered separately.

Brands A and C synthetic agents influenced the air void system adversely. The effects were similar to the observations made with brand D. SSA and SSC produced larger spacing factors and lower strengths than the Vinsol resin agents in their own brand categories SSA and SVC1, SVC2 respectively. Air bubble

distributions for these samples are given in Figs. 20 and 22. Magnified images of the air bubble system for these samples are compared in Figs. 26 and 27.

Quantitative evidence was presented through bubble distribution and air void parameters. Qualitatively, from the magnified images, it can be observed that the larger bubble samples produce the weaker concretes.

In general, the following percent strength losses were observed in series-II synthetic air entrained concretes:

- Strength loss of 12.6% for SSA in comparison with SVA.
- Less than 0.1% strength loss for SSB in comparison with SVB.
- Strength loss of 6.5% for SSC in comparison with SVC1.
- Strength loss of 10.2% for SSC in comparison with SVC2.
- Strength loss of 6.0% for SSD1 in comparison with SVD1.

Results described above suggest direct correlation between the size of the air bubbles and the compressive strength in the air-entrained concretes.

Production of larger air bubbles by the Synthetic admixtures in all cases resulted in reduction of compressive strength as demonstrated by SSA, SSC, and SSD1. However, SSB, a Synthetic agent, did not produce bubbles larger than those observed in SVB, its Vinsol resin counterpart, and therefore it also did not exhibit a reduction in compressive strength. As described in the earlier sections of this report, air-entraining admixtures are surface-active agents and the manner by which they facilitate production of air bubbles in concrete is through reduction of surface tension in water. Therefore, it is important to analyze and compare the effects of the two different types of admixtures on the surface tension characteristics of concrete mixtures. This is accomplished in the following section.



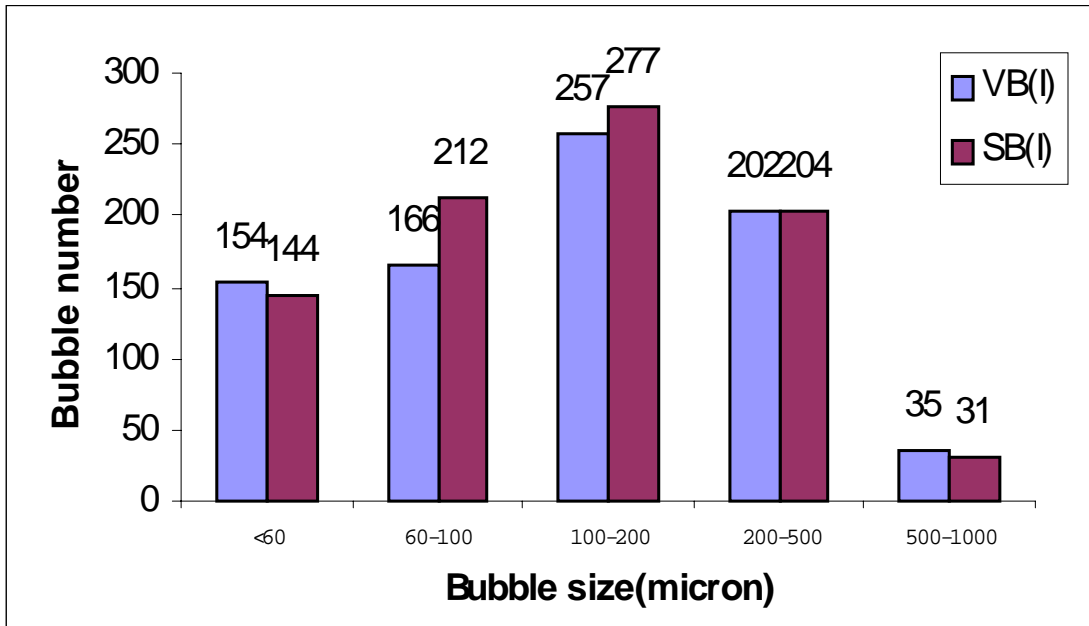


Figure 11 Comparison of air void sizes for brand B admixtures (group-I measurements)

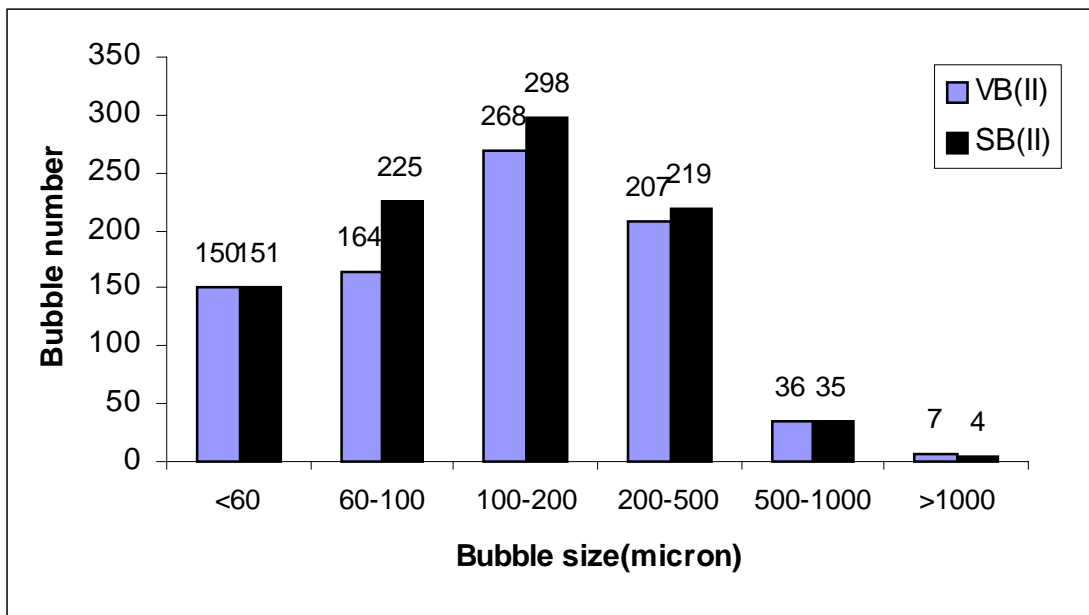


Figure 12. Comparison of air void sizes for brand B admixtures (group-II measurements)

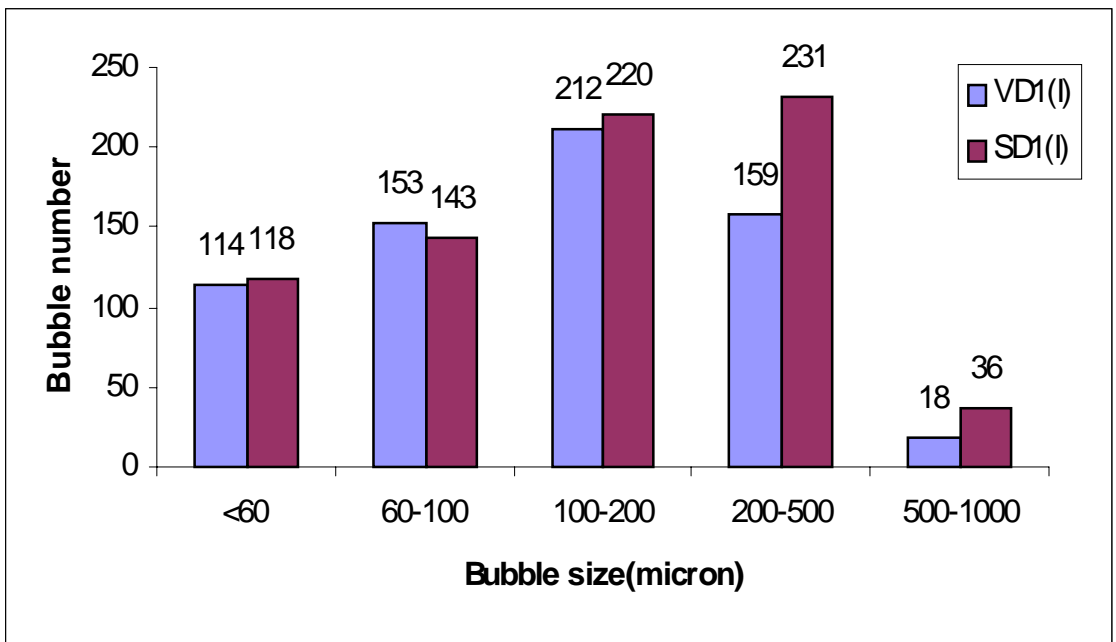


Figure 13. Comparison of air void sizes for brand D admixtures (group-I measurements)

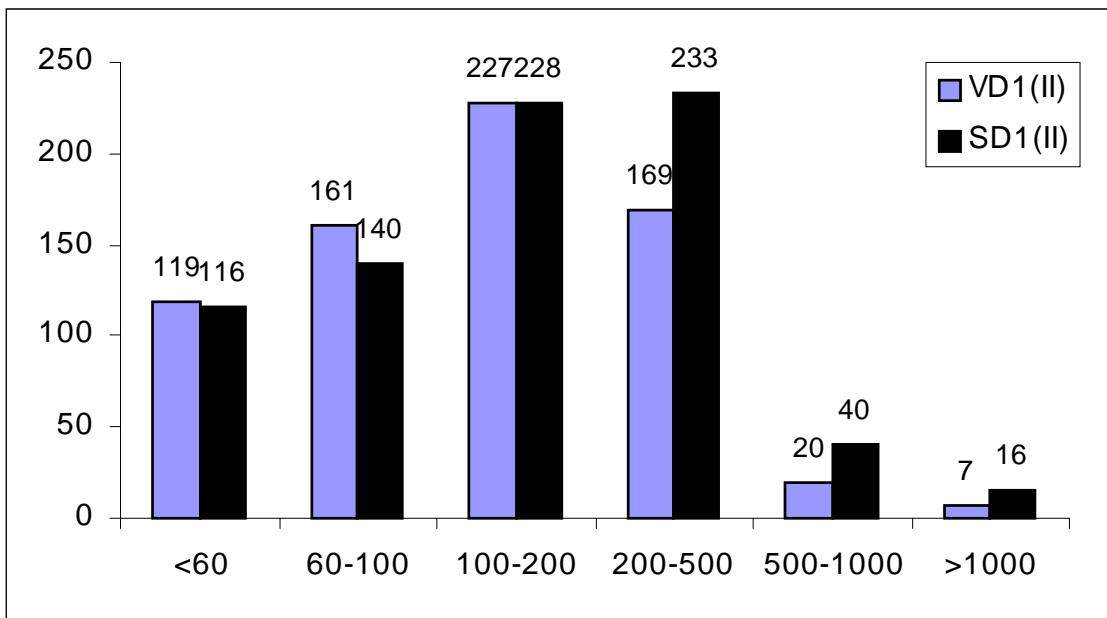


Figure 14. Comparison of air void sizes for brand D admixtures (group-II measurements)

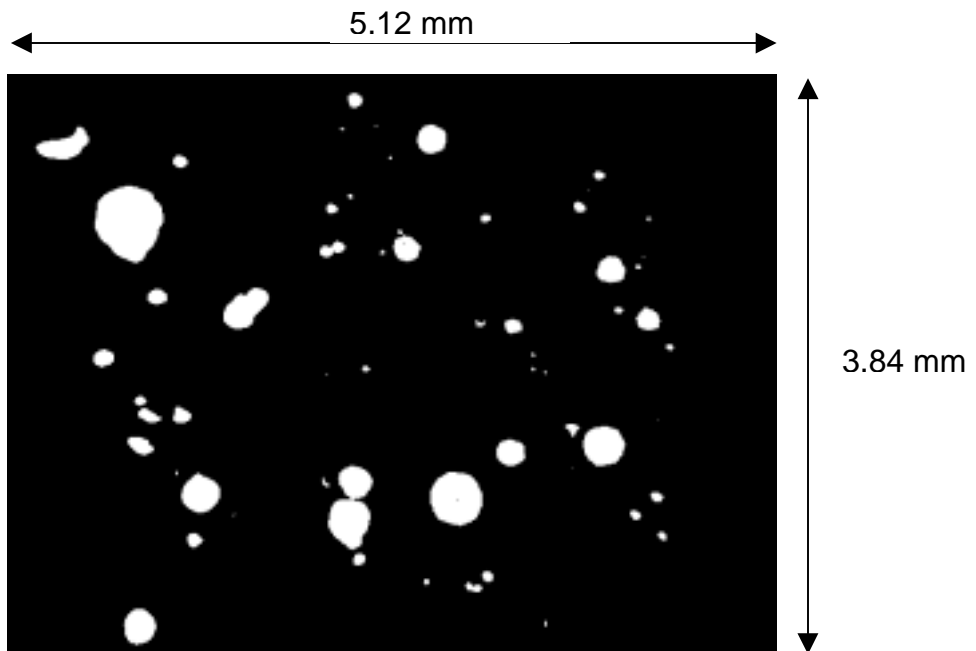


Figure 15. Magnified image of air bubbles in VB

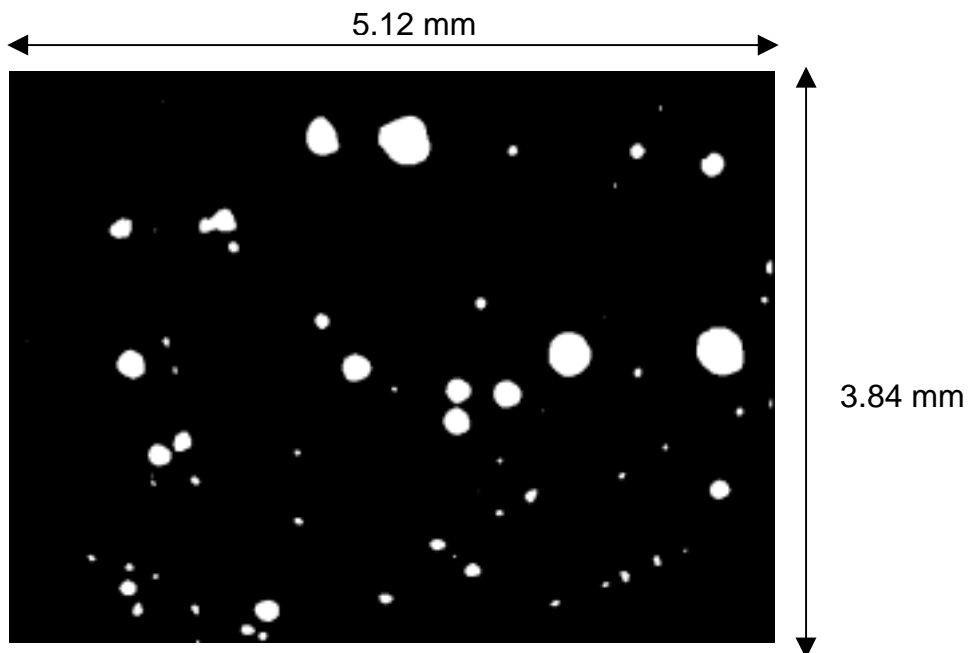


Figure 16. Magnified image of air bubbles in SB

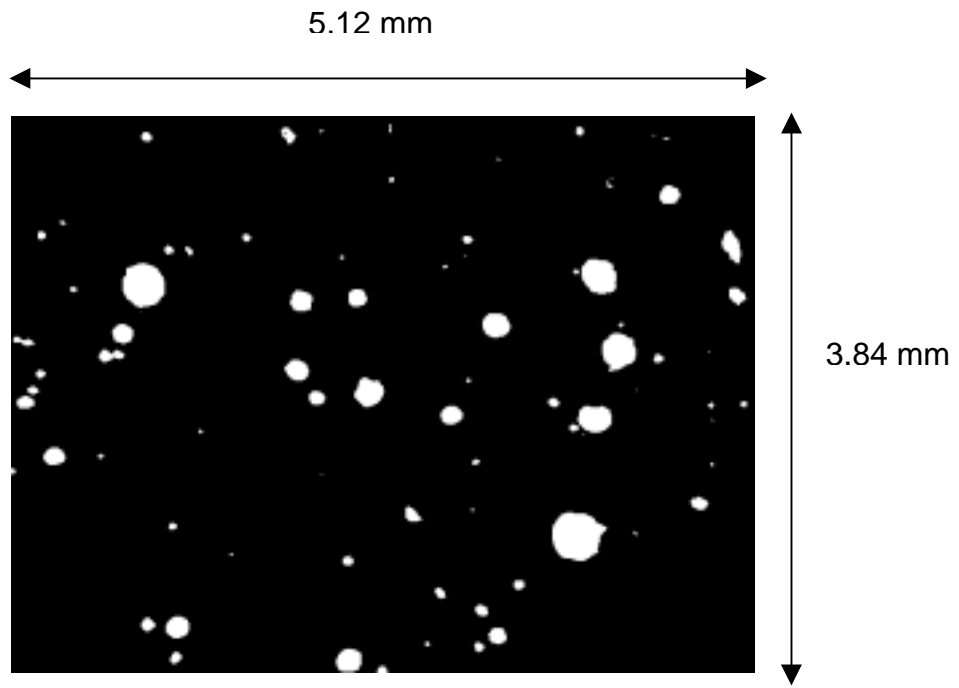


Figure 17. Magnified image of air bubbles in VD1 (Magnification 52X)

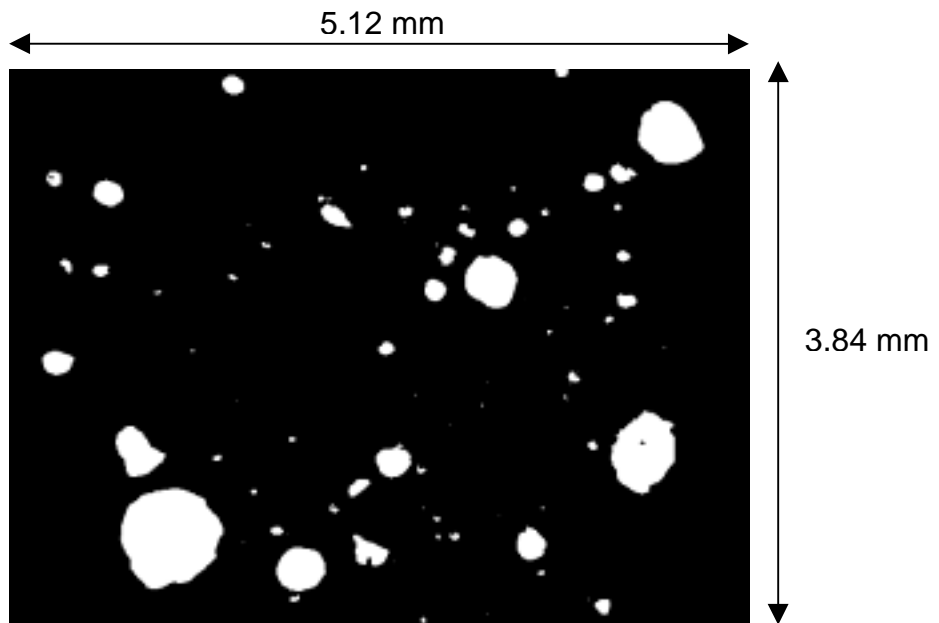


Figure 18. Magnified image of air bubbles in SD1 (Magnification 52X)

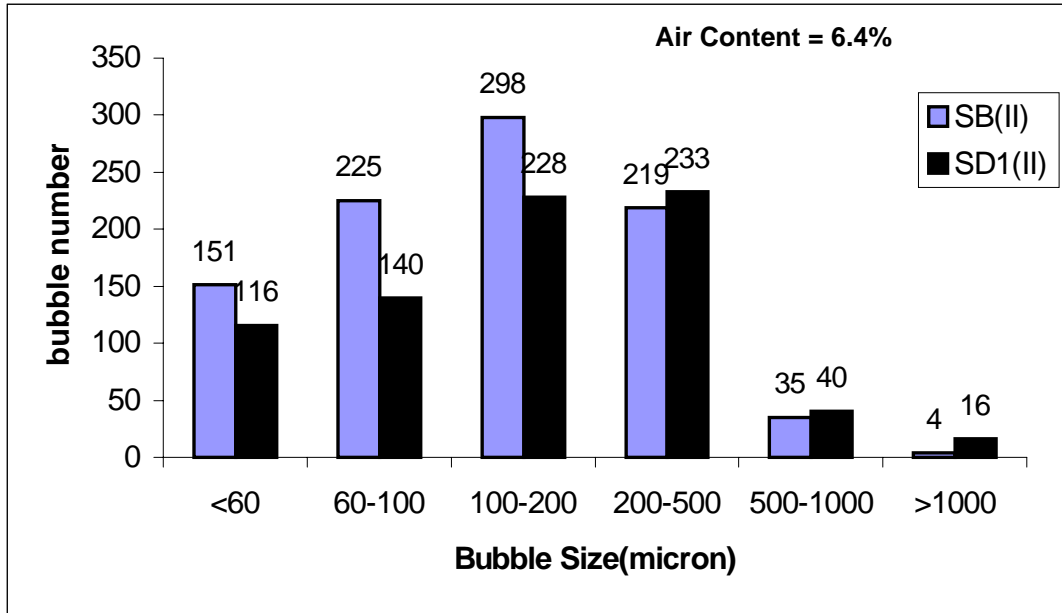


Figure 19. Comparison of air void distributions in concretes produced with two different brands of synthetic air entraining admixtures (Series-I).

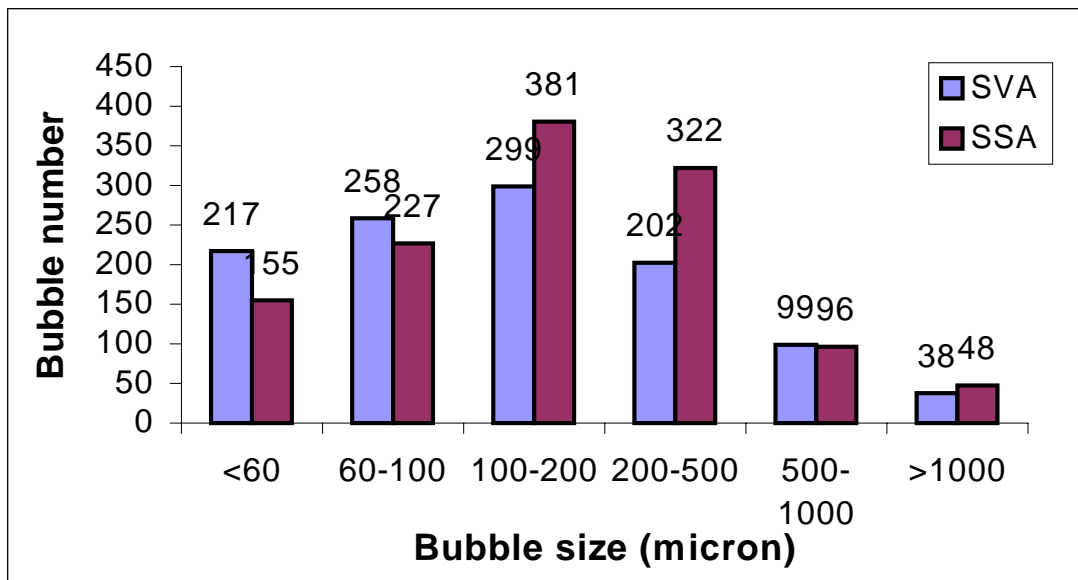


Figure 20. Comparison of air void size distribution for brand A admixtures (Series-II)

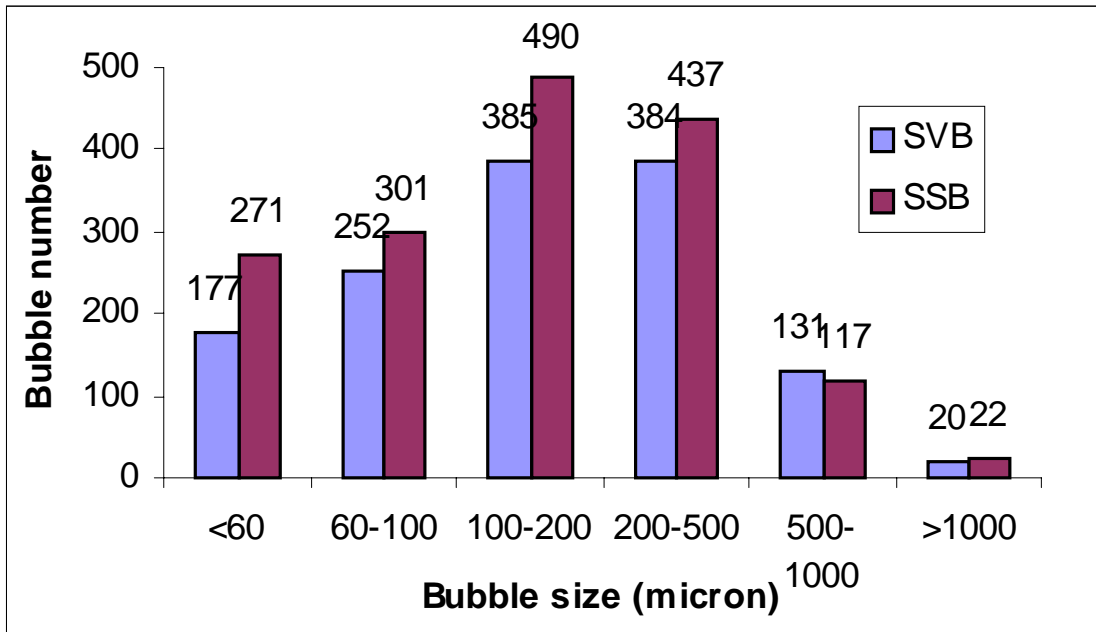


Figure 21. Comparison of air void size distribution for brand B admixtures (Series-II)

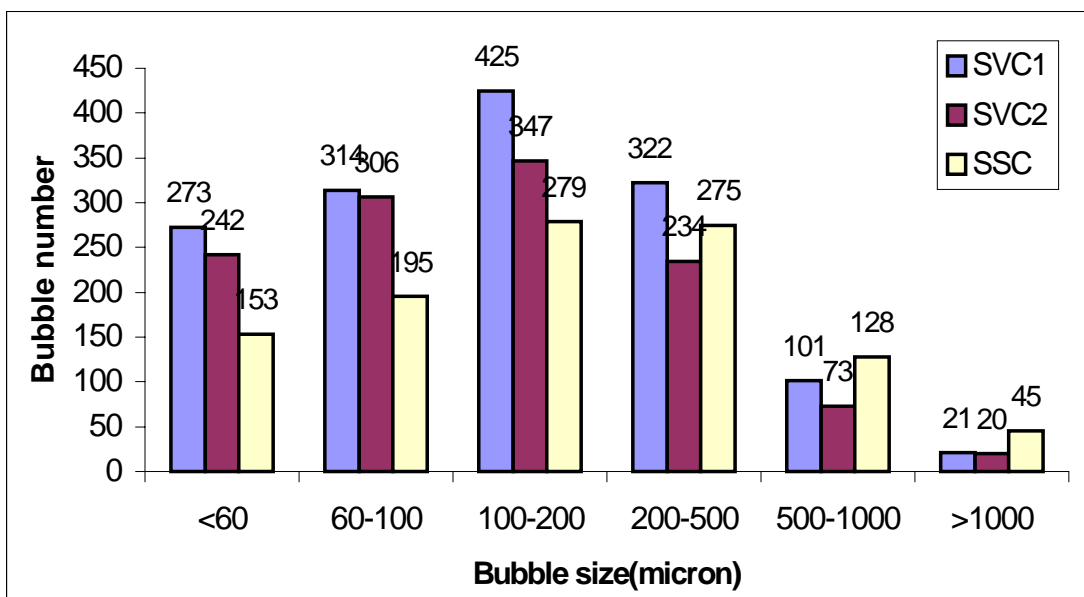


Figure 22. Comparison of air void size distribution for brand C admixtures (Series-II)

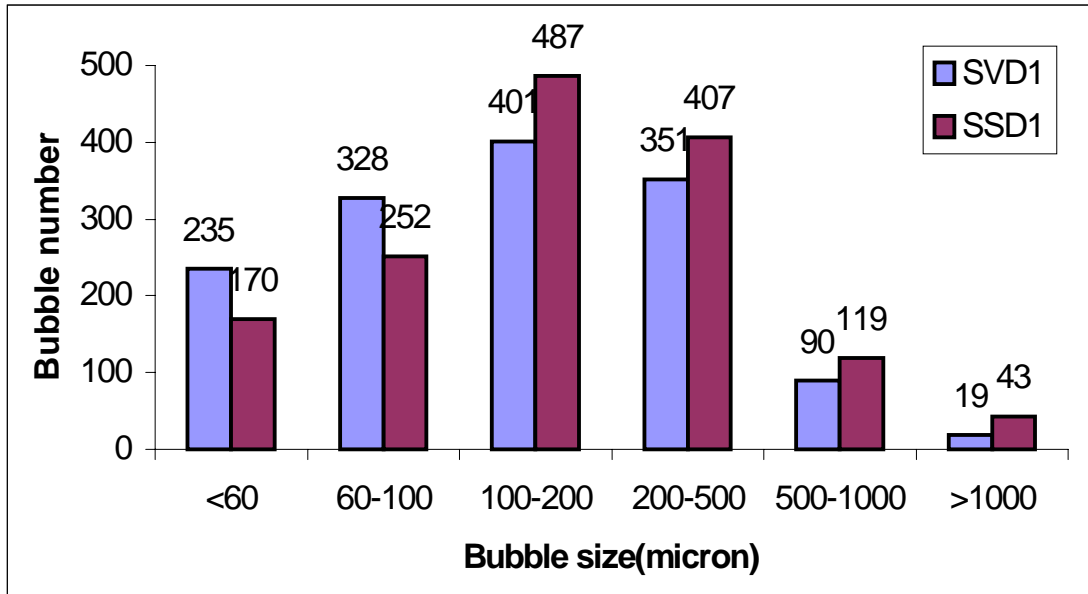
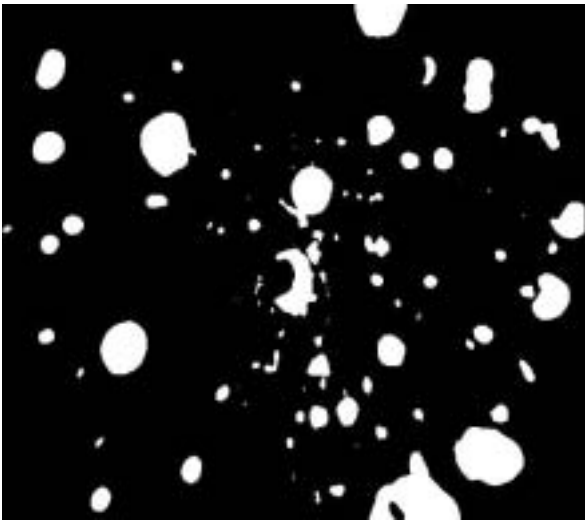


Figure 23. Comparison of air void size distribution for brand D admixtures (Series-II)



SVB



SSB

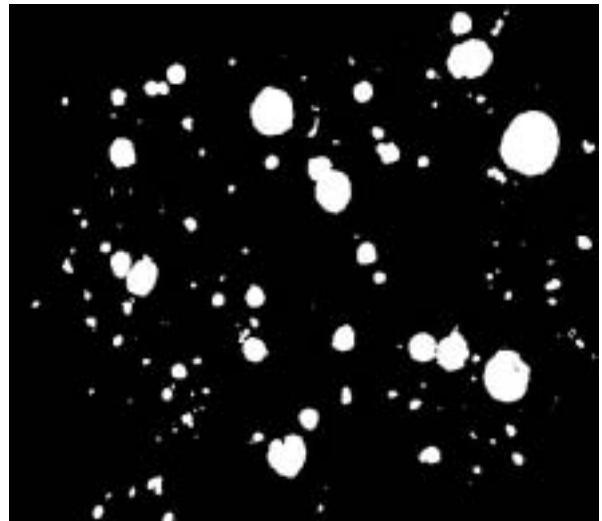
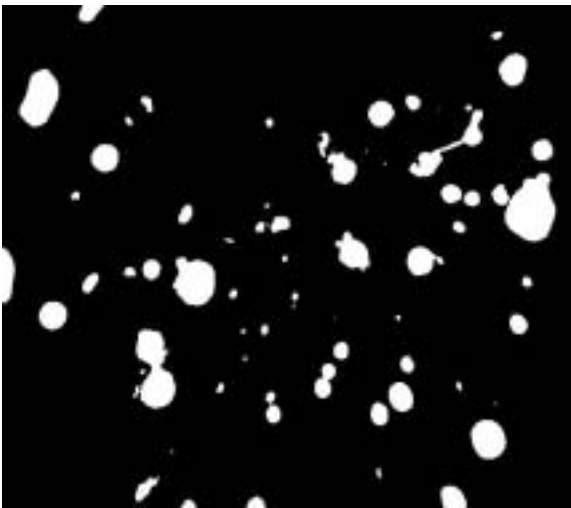


Figure 24. Magnified images of air bubbles in SVB and SSB (Magnification 52X)

SVD1



SSD1



Figure 25. Magnified images of air bubbles in SVD1 and SSD1 (Magnification 52X)

SVA

SSA

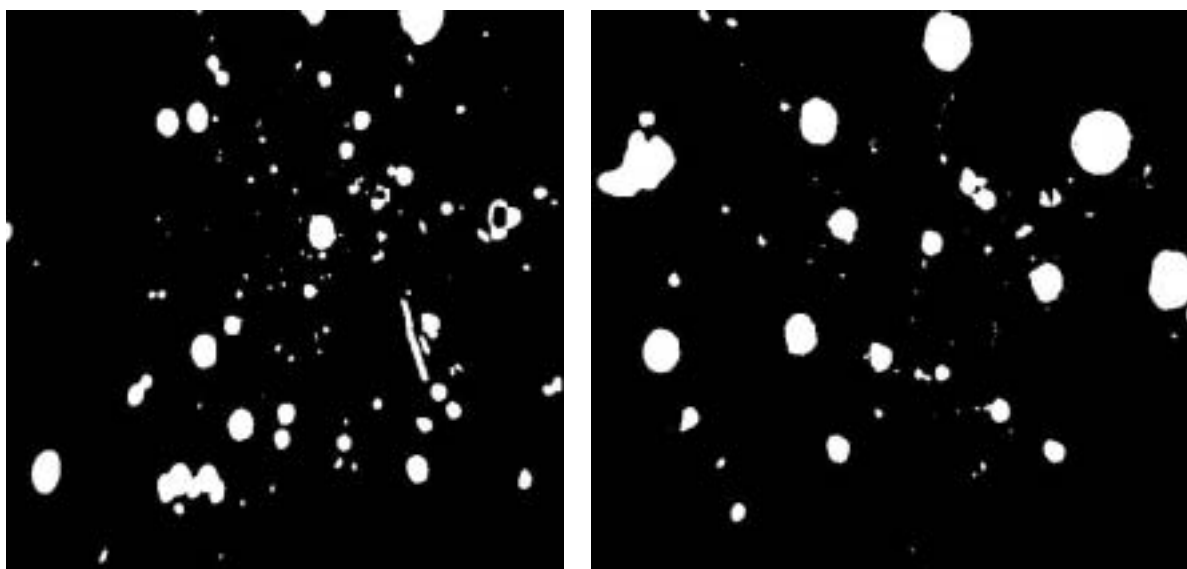


Figure 26. Magnified images of air bubbles in SVA and SSA (Magnification 52X)

SVC1

SVC2

SSC

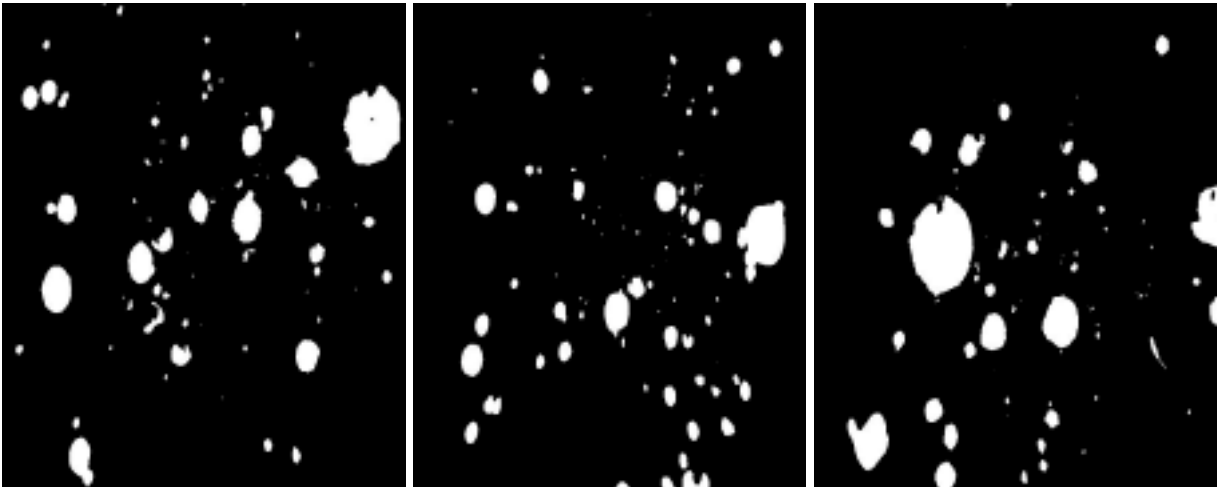


Figure 27. Magnified images of air bubbles in SVC1, SVC2 and SSC  
(Magnification 52X)

## Analysis of Surface Tension Data

Results from the measurement of surface tension in water as well as cement filtrates are given in table 27. As described earlier, three replicate measurements were made per sample, and a standard deviation of less than 0.2 dyne/cm was achieved for all the samples. For the four brands of admixtures, the measured surface tensions of Vinsol and synthetic agents in solutions of water are compared in Fig. 28. In comparison to Vinsol resins, the Synthetic agents, irrespective of brand were more effective in lowering the surface tension of water. This could explain capability for creation of more and larger air voids in concretes containing Synthetic agents. However, these results did not explain the behavior of brand-B synthetic agent, as in terms of air void distribution it performed better than the Vinsol concrete both in series-I and II tests. It was hypothesized that the surface tension lowering capability of certain admixtures is influenced by the presence of cement, and in this case in a positive manner. Therefore, it was decided to perform additional tests, mainly to measure the surface tension of the solutions containing cement filtrates.

The next series of experiments as described in the experimental procedure section of this report pertained to the measurement of surface tension in cement filtrates containing the admixtures. Comparison of results for the various brands and admixture types is given in Fig. 29. As shown in this figure, except for brand-B, other synthetic agents were more effective in lowering the surface tension of cement filtrate than their Vinsol resin counterparts. Moreover, for brand-C, the surface tension in the filtrate containing Vinsol-I was lower than the one for synthetic and Vinsol-II. This explains existence of larger bubbles in concretes manufactured by Vinsol-I as noted previously. In addition, in comparison to the synthetic cement filtrates, smaller size bubbles were produced in Vinsol-I cement filtrates and this explains the higher specific surface for the concretes containing Vinsol-I. The synthetic agent produced more of the larger bubbles (specific surface =  $15 \text{ mm}^{-1}$ ), and this explains the lower compressive strength.

As described earlier, lower surface tensions give rise to production of more bubbles and it seems that in concretes it facilitates stability for larger air bubbles. These results are commensurate with the air bubble size and compressive strength data presented earlier. Concretes containing the brand-B synthetic air-entraining agent produced smaller air bubbles, whereas all the other synthetic agents produced concretes with larger air bubbles with strengths lower than their Vinsol resin counterparts. Brand-B's synthetic concrete possessed compressive strengths comparable to Vinsol resin concretes. Although surface tension plays a significant role in the formation of the larger bubbles, however, lower surface tensions measured in Vinsol-I cement filtrates did not prohibit formation of sufficient number of smaller bubble sizes to balance the overall number of bubbles including the larger ones in the concrete. In fact, the compressive strength of Vinsol-I at higher air content (by volume) was higher than the

synthetic concrete for brand-C. It may be concluded that, the synthetic agents lower while surface tension plays a significant role in production of all sizes of bubbles, other factors may be responsible for creation of large bubbles and prevent formation of smaller bubbles in synthetic admixtures. More extensive research is needed to completely understand this phenomenon.

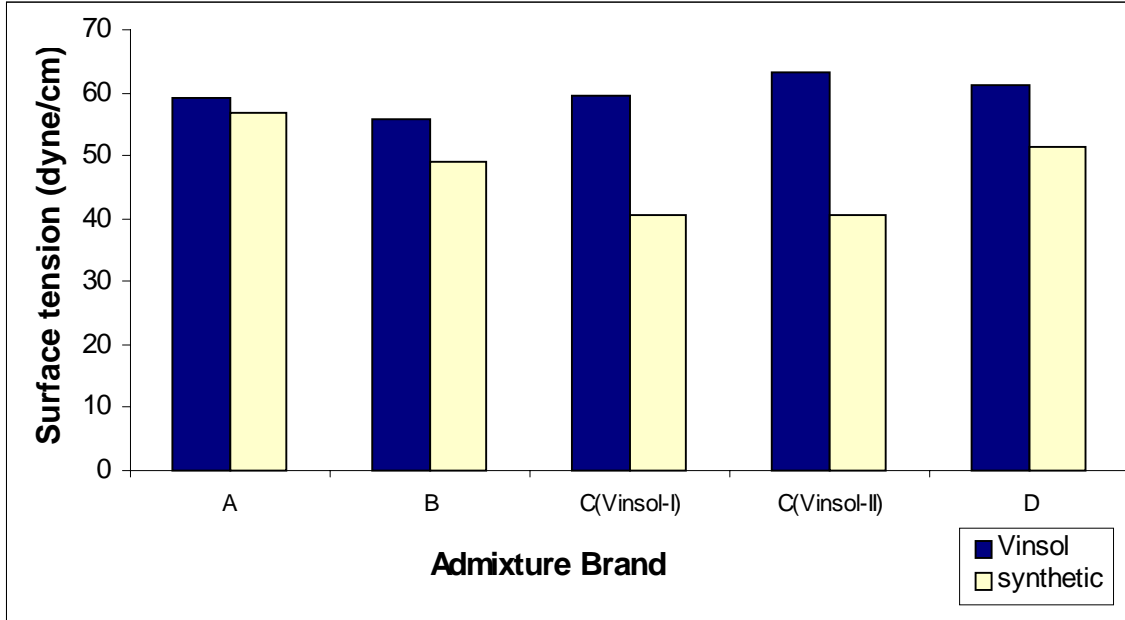


Figure 28. Surface tension of air entraining agent in water solution

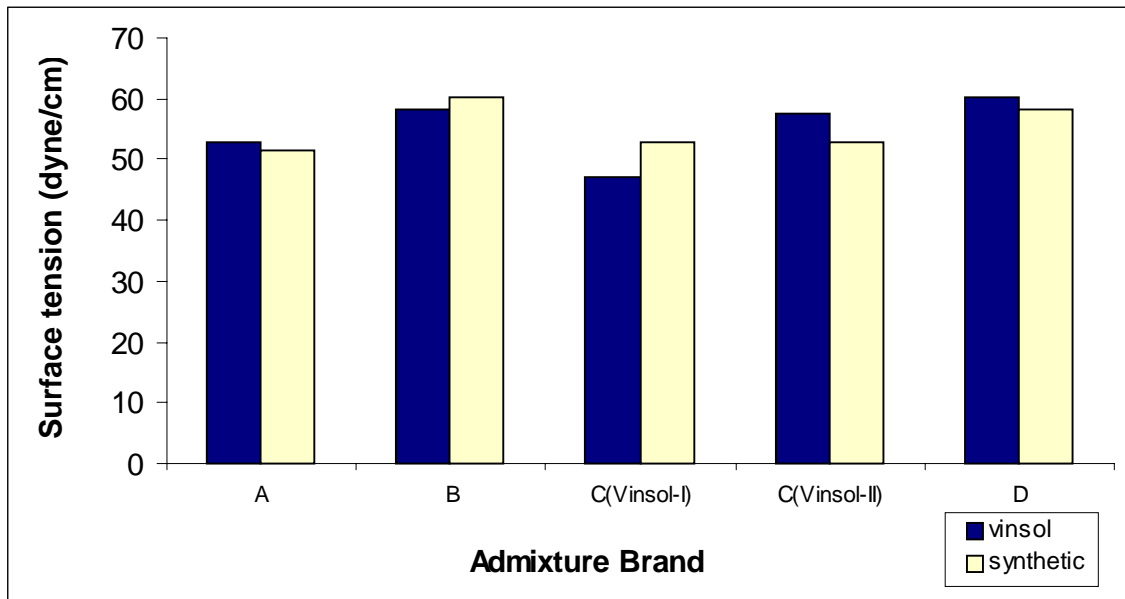


Figure 29. Surface tension of filtrate of cement paste

## Higher Dosages of Admixtures

Comparison of surface tension data for the synthetic and Vinsol resin brand D admixture at various dosages are given in table 28 and Figs. 30 and 31. As shown in these figures, increased dosages of the Vinsol resin admixture consistently decreased the surface tension of the water as well as the cement filtrate solutions. On the other hand, for both the water and cement filtrate solution; increasing levels of synthetic admixture from 1 to 2 ounces resulted in an increase in surface tensions. Whereas, the increase in dosage of the synthetic agent from 2 to 4 ounces was associated with decrease in surface tensions of the water and cement filtrate solutions.

Examination of air contents, air void parameters and compressive strengths for specimens manufactured at these higher dosages provide information consistent with the surface tension data. As shown in table 26, for Vinsol resins, the specific surfaces decreased from  $20\text{-mm}^{-1}$  for SVD1 to  $16\text{-mm}^{-1}$  for SVD2, and  $15\text{-mm}^{-1}$  for SVD3 indicating presence of larger air bubbles for increasing levels of the admixture. Consistent with the surface tension data, except at the dosage level of 1-ounce, for higher dosages, the air bubbles generated by the Vinsol resin are larger than the ones generated by the synthetic agent (specific surface of 21 for SSD2, and 17.8 for SSD3). Figs 32 and 33 pertain to the magnified images of the air bubbles in these samples. Moreover, comparison of compressive strength data from table 23 for these specimens further demonstrates the correspondence between the surface tension data and the compressive strength. As shown in this table, the compressive strength of the concretes containing 1-ounce of the Vinsol admixture was higher than the concretes containing 1-ounce of the synthetic admixture. For the concretes containing higher dosages of brand-D admixture, the reverse is true, where the synthetic admixture concretes exhibited higher compressive strengths.



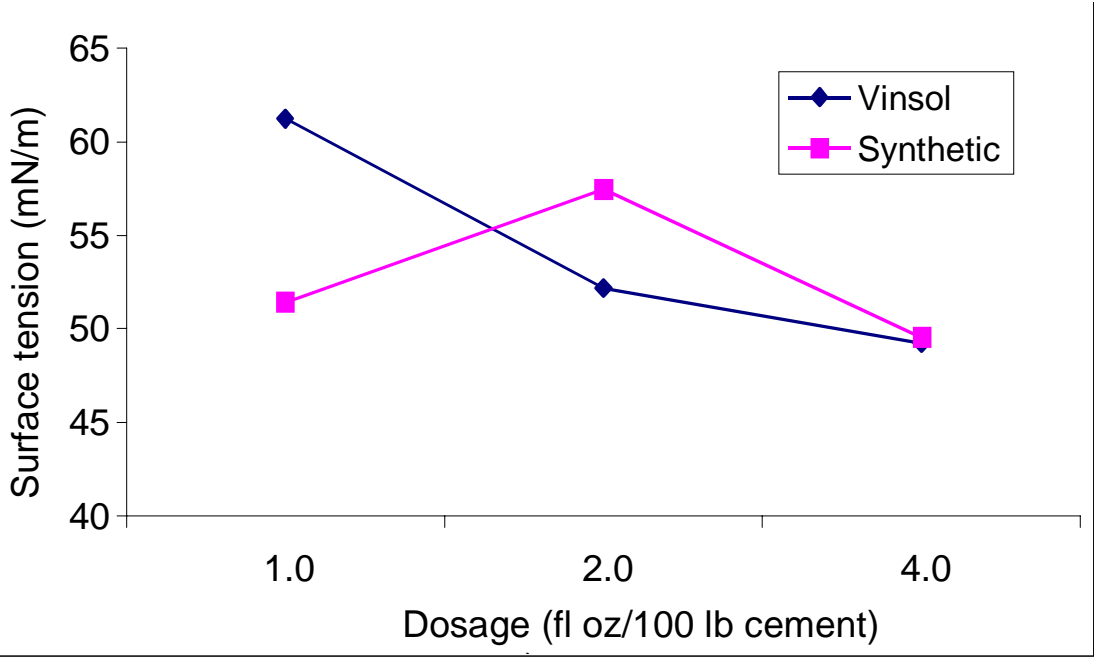


Figure 30. Surface tension of Brand-D water solution

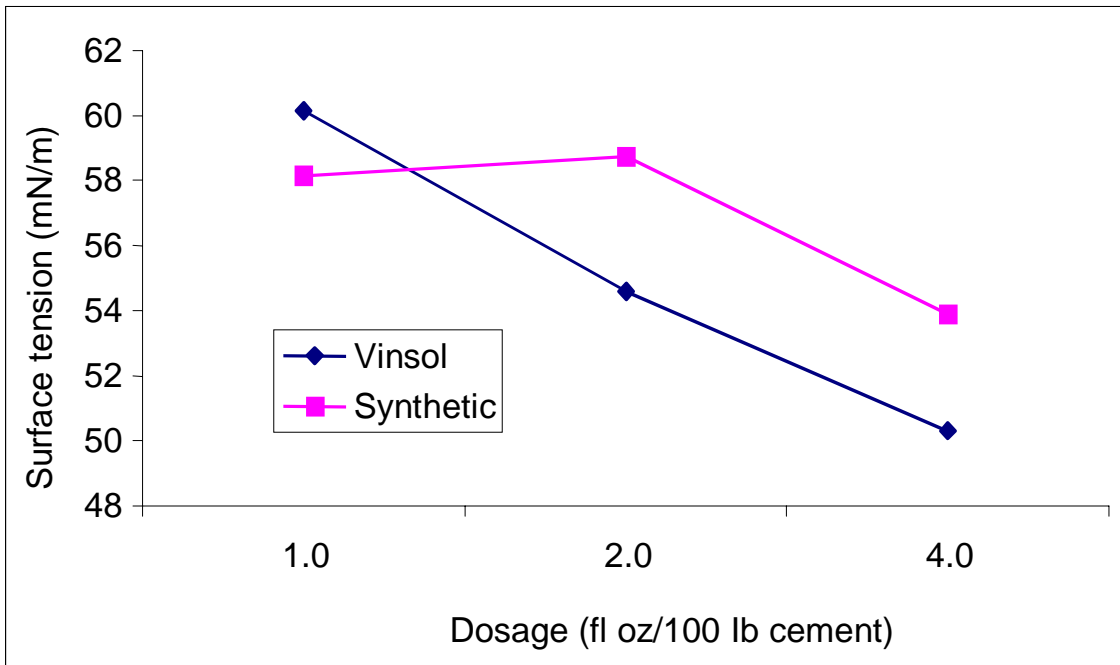
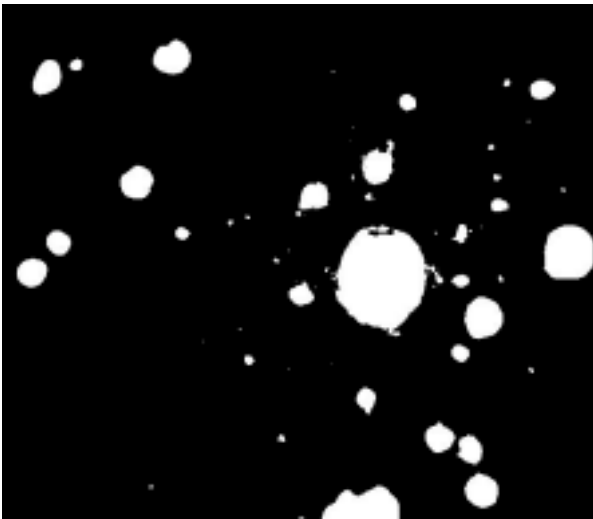


Figure 31. Surface tension of Brand-D filtrate of cement paste

SVD2



SSD2

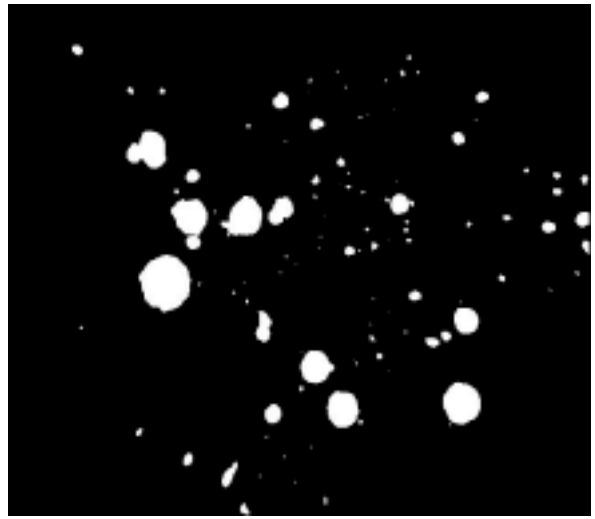
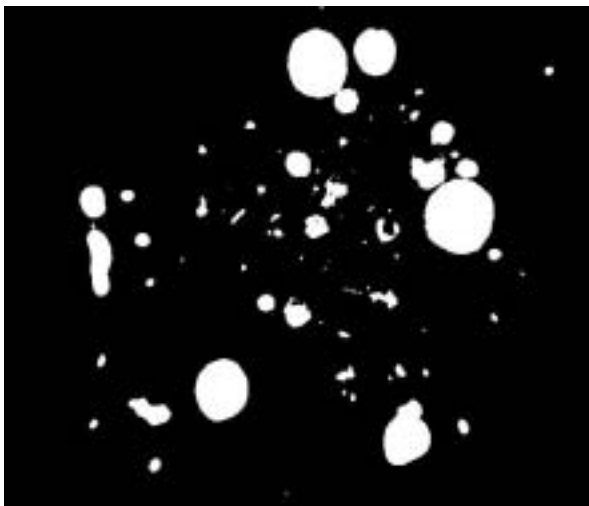


Figure 32. Typical surface image of samples SVD2 and SSD2

SVD3



SSD3

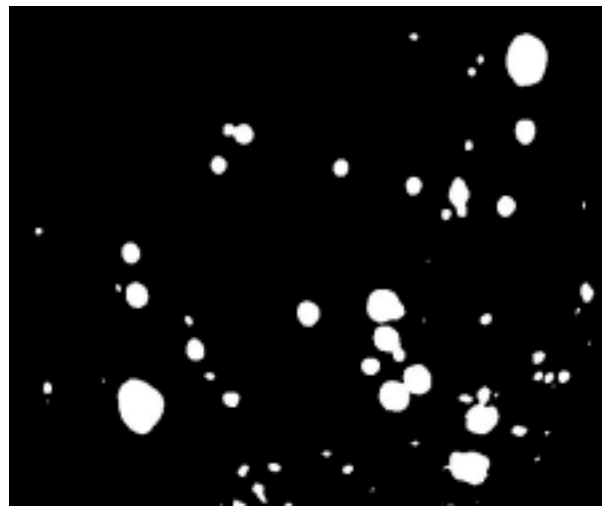


Figure 33. Typical surface image of samples SVD3 and SSD3

## CONCLUSIONS

A research program was undertaken through which it was possible to gain knowledge as to the reasons behind the loss of compressive strength in concrete normally associated with the use of synthetic air-entraining admixtures. The research program involved four different brands of admixtures, and two different types of admixtures per brand. Brand-C manufactured two different types of Vinsol resins and both were examined in this investigation. Brands B and D were tested in mixtures containing WRA as well as those with HRWA. While the primary objective of the research program was to investigate all the admixtures at normally recommended dosages, additional tests were performed for higher dosages for the agents manufactured by brand-D. The experimental program involved determination of compressive strength, measurement of air content at fresh state, detailed determination of air void parameters at the hardened state, and measurement of surface tension of admixtures in water and cement filtrates. Summary of specific findings of the research based on the experimentation with the four different brands of admixtures at normally recommended dosages is stated below:

1. Concretes produced by the synthetic air entraining admixtures, in general exhibit lower compressive strengths than those produced by Vinsol resin agents.
2. The primary reason for the strength loss associated with the Synthetic air-entraining admixtures is creation of larger air bubbles (voids) by these admixtures.
3. In general, synthetic air entraining admixtures increase the surface-tension-reduction capability of the cementitious mixture, giving rise to creation of larger bubbles.
4. The effect and severity of air entraining admixtures on strength loss, and air void distribution is brand sensitive. Generalization in terms of strength loss and air void distribution for synthetic admixtures will lead to erroneous results.
5. For brand-B, both the synthetic as well as the Vinsol admixtures created concretes with identical compressive strengths. Examination of the air void parameters indicated identical air bubble size distributions and even slightly smaller bubble sizes in the concretes produced by the synthetic agent.
6. The only exception to the correlation between the surface tension and the strength pertain to the Vinsol resin-I of brand-C that was more effective than its synthetic counterpart in reducing the surface tension

of the mixture, but exhibited slightly larger strengths than the concrete produced by the synthetic admixture.

7. Examination of brand-D at higher dosages further confirmed the existence of correlation between the surface tension, bubble size distribution in hardened concrete and compressive strength. In this case, increased levels of Vinsol resin admixtures was associated with strength loss, whereas, increasing the dosage of synthetic admixtures, first increased the compressive strength and then reduced it.

## **RECOMMENDATIONS**

The findings summarized above are based on reasonable number of experiments. However, novelty of results requires further experimentation with a variety of cement brands and mixture proportions. The results reported here do not preclude the use of synthetic agents for entrainment of air in concretes. However, it seems that the interaction between cementitious mixtures and synthetic air entraining admixtures are not quite understood and more data is needed for proper proportioning of the synthetic admixture in concretes. Based on the results of the present study, the following recommendations may aid NJDOT in reducing the compressive strength loss in air-entrained concretes:

1. Under equal circumstances and availability Vinsol resin admixtures are more favorable due to the established compatibility of mixtures with Vinsol resins.
2. With the limited number of brands tested here, and if the price and availability dictates the use of synthetic admixtures, brand-B shall be used as it did not cause any compressive strength losses.
3. As stated in the conclusion section of this report, results are brand sensitive and development of correlation relationships between loss of strength and the use of synthetic agents is brand sensitive and will lead into erroneous results. It is possible to establish such relationships based on availability of data with information as to the brand, type, dosage and compressive strength. As per the findings of this study, such relationships need to be established per brand as the results were brand sensitive. Sufficient amount of data is necessary to develop statistically viable relationships.

## **APPENDIX-A: AUTOMATED LINEAR ANALYSIS SYTEM**

During the course of this project, an automated image analysis system for the determination of air void parameters of concrete including the size and spacing of air bubbles has been developed. Hardware and software were developed in order to fully automate and furthermore optimize the linear traverse method as stipulated by ASTM C-457. The new system automatically generates the bubble size distribution as well as the total air content, specific surface and spacing factor for concrete samples.

### **Methodology**

The system is intended to integrate motor-driven stage, video camera, image acquisition, real time image analysis software and user interface together and thus to implement fully automated linear traverse method.

### **Sample Preparation**

Concrete slices are cut from the well-cured concrete cylinders or cores. Their surfaces are lapped with successively finer abrasives (Aluminum Oxide and silicon carbide) until they are suitable for microscopical observation (Figure 34, 35). The stamp pad ink is used to paint the polished surface and to produce totally black surface. After drying, white paste (e.g. zinc oxide compound) is applied and pressed on the same surface and pressed to ensure all surface voids are all properly filled. The surface is carefully cleaned to produce sharp contrast between air voids and the matrix (Figure 36, 37).

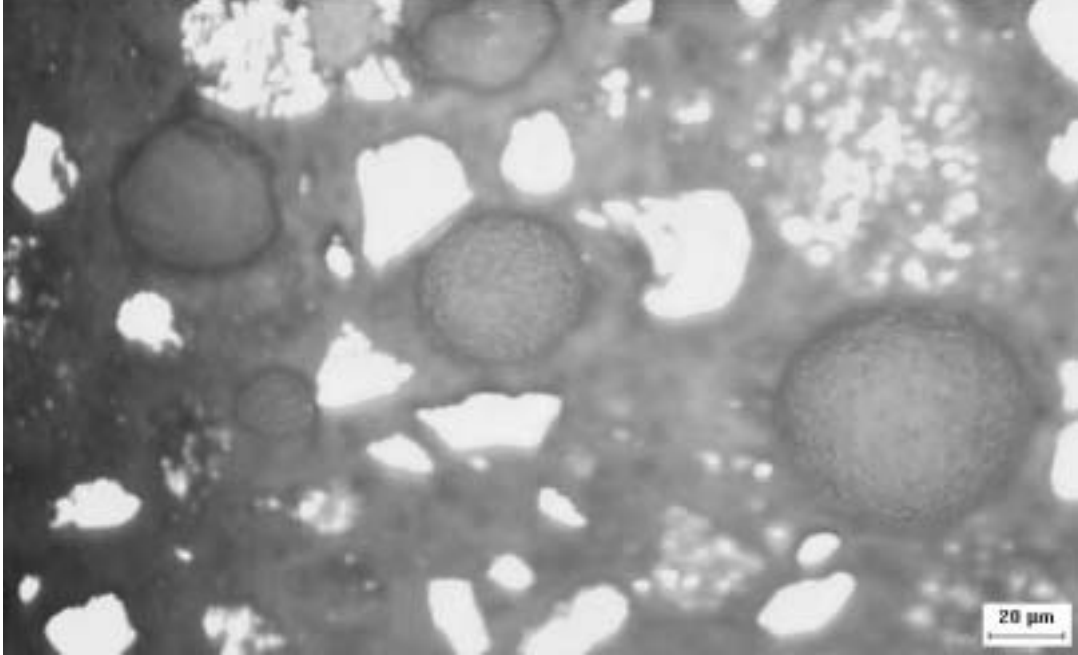


Figure 34. Concrete surface after proper lapping (1)

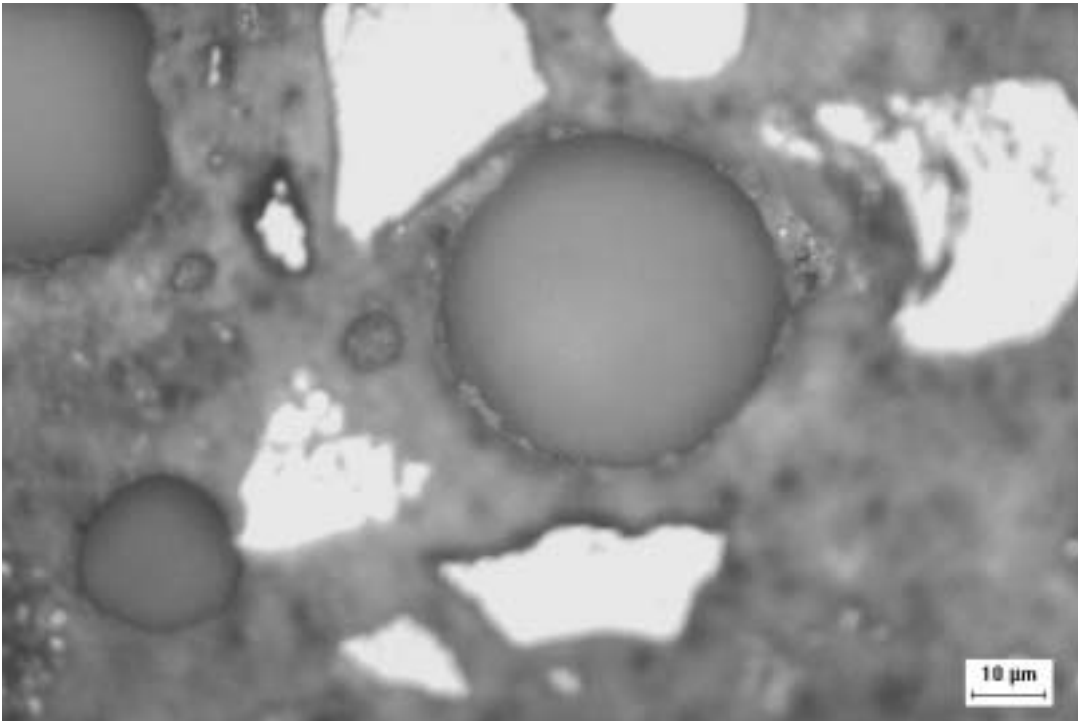


Figure 35. Concrete surface after proper lapping (2)

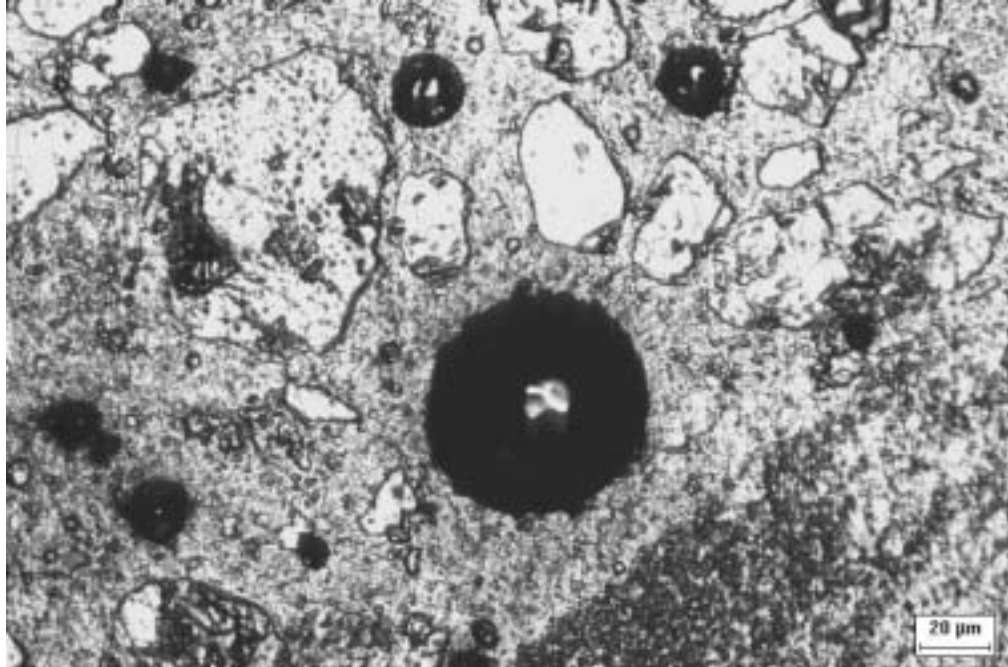


Figure 36. Concrete surface after proper painting (1)

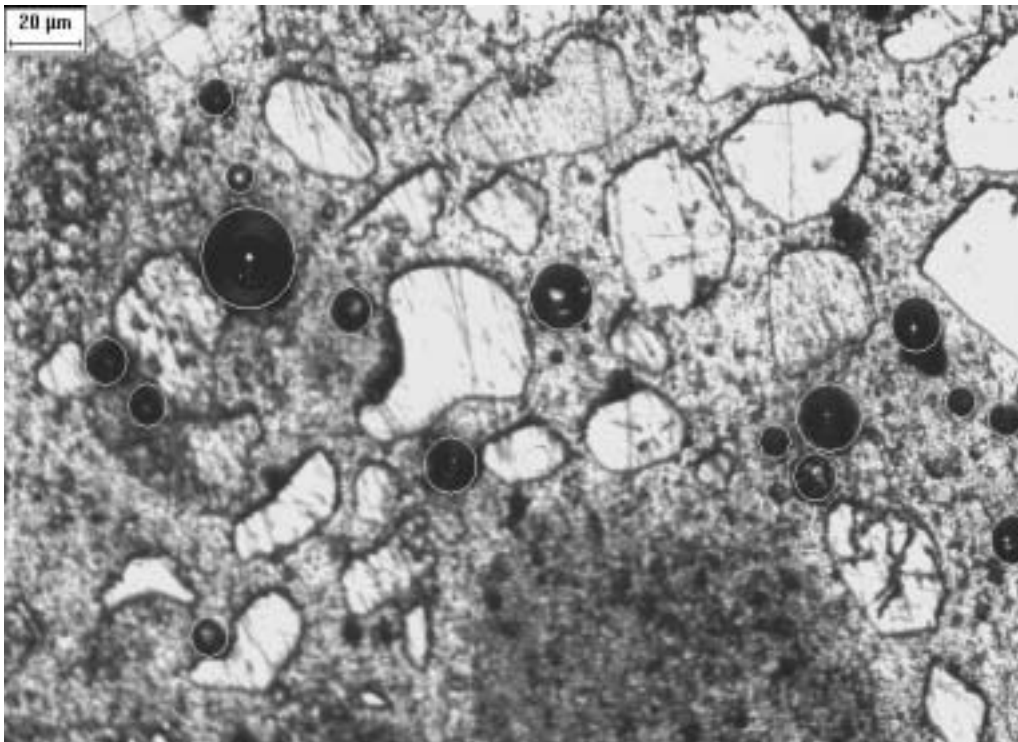


Figure 37. Concrete surface after proper painting (2)



## Description of the system

The system employs the variation between the dark and white pixels as well as the shape of the air voids for recognition and measurement of air void parameters. The system is automated and runs unattended and measures the parameters required by ASTM C-457 once the prepared sample is inserted into the equipment.

The system consists of:

- A microscope fitted with a digital video camera and a motorized platform that moves the concrete sample over a preprogrammed measurement path.
- An image analysis program that processes the data from the microscope and measures the diameter of individual air bubbles, and the spacing between them. It differentiates the air bubbles from other voids in the concrete. The routines use the measured air bubble data for computation of air-void parameters required for the determination of concrete properties.

The schematic diagram showing the various system elements is shown below (Fig. 38).

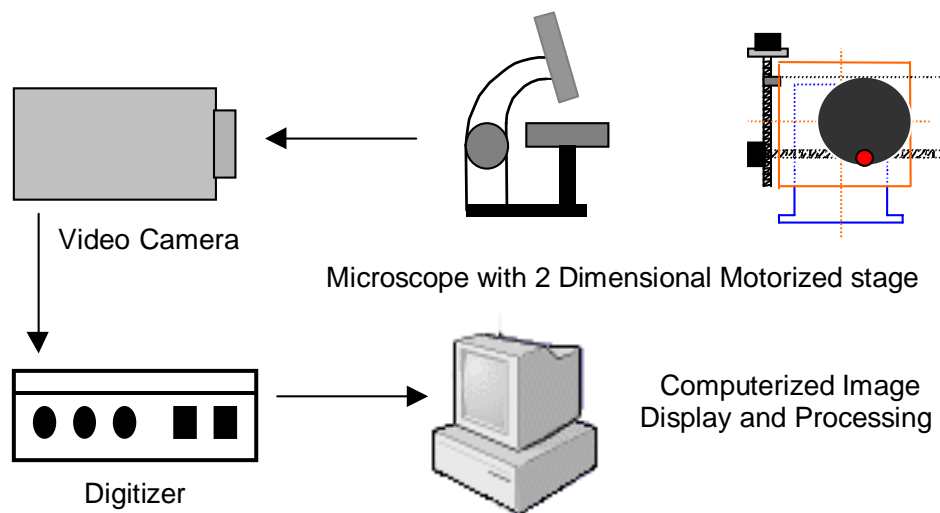


Figure 38. Configuration of system

Output of the system corresponding to a typical linear traverse run is depicted in (Fig. 39)

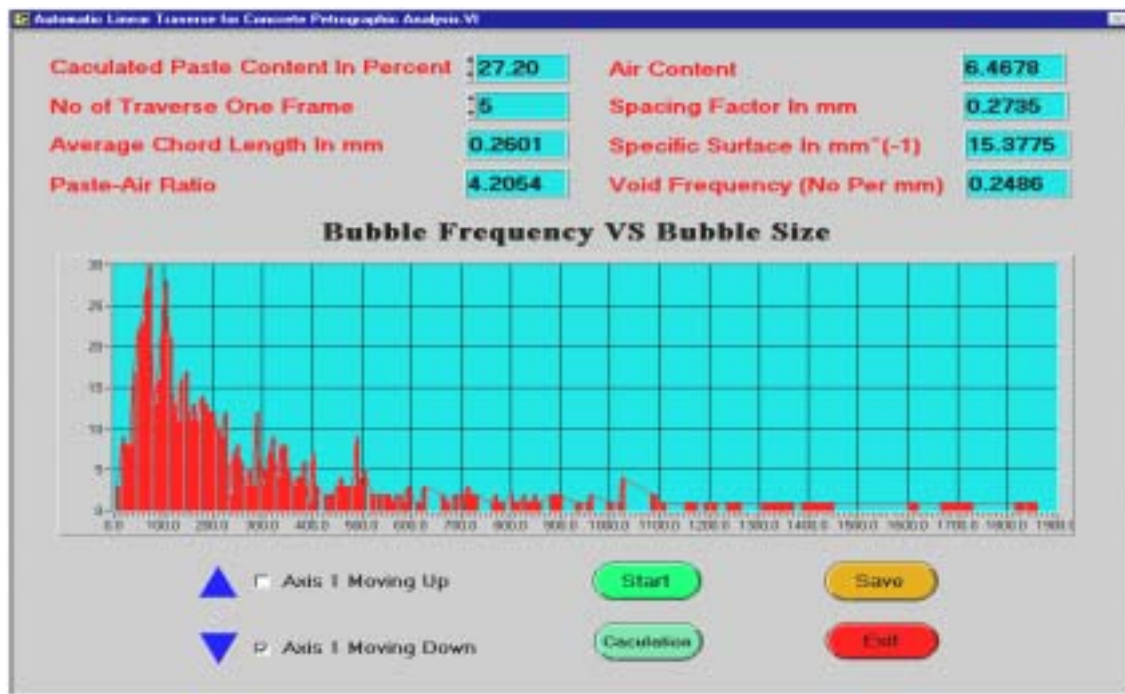


Figure 39. View of computer screen

### System Reliability and Repeatability

Two hardened concrete samples were prepared and multiple measurement sets were conducted on each. The automated test results were comparable to the ASTM 457 standardized method. The results using the automated test method are reproducible and are shown in tables 29 and Figures 40 and 41.

Table 29. Results from automated tests are Comparable to ASTM C 457

Sample No.	Paste-air ratio	Air content	Spacing factor (mm)	Specific Surface (mm <sup>-1</sup> )	Void Frequency (No./mm)	Average Chord Length, (mm)
Sample 1						
<b>ASTM C457</b>	3.8774	7.0150	0.2131	18.1984	0.3191	0.2198
<b>Auto1-1</b>	4.0352	6.7407	0.2539	15.8918	0.2678	0.2517
<b>Auto1-2</b>	3.9777	6.8380	0.2456	16.1928	0.2768	0.2470
<b>Auto1-3</b>	4.4209	6.1526	0.2580	16.9711	0.2610	0.2357
<b>Auto1-4</b>	4.3318	6.2791	0.2508	17.2752	0.2712	0.2315
<b>Auto Mean</b>	4.1914	6.5026	0.2521	16.5827	0.2692	0.2415
Sample 2						
<b>ASTM C457</b>	4.5663	5.9567	0.2485	18.3739	0.2736	0.2177
<b>Auto2-1</b>	4.8322	5.6289	0.2581	17.6694	0.2486	0.2264
<b>Auto2-2</b>	4.5757	5.9444	0.2623	16.9590	0.2520	0.2359
<b>Auto2-3</b>	4.9924	5.4483	0.2524	18.3377	0.2498	0.2181
<b>Auto2-4</b>	4.7371	5.7419	0.2628	18.7758	0.2524	0.2130
<b>Auto Mean</b>	4.7844	5.6909	0.2589	17.9355	0.2507	0.2234

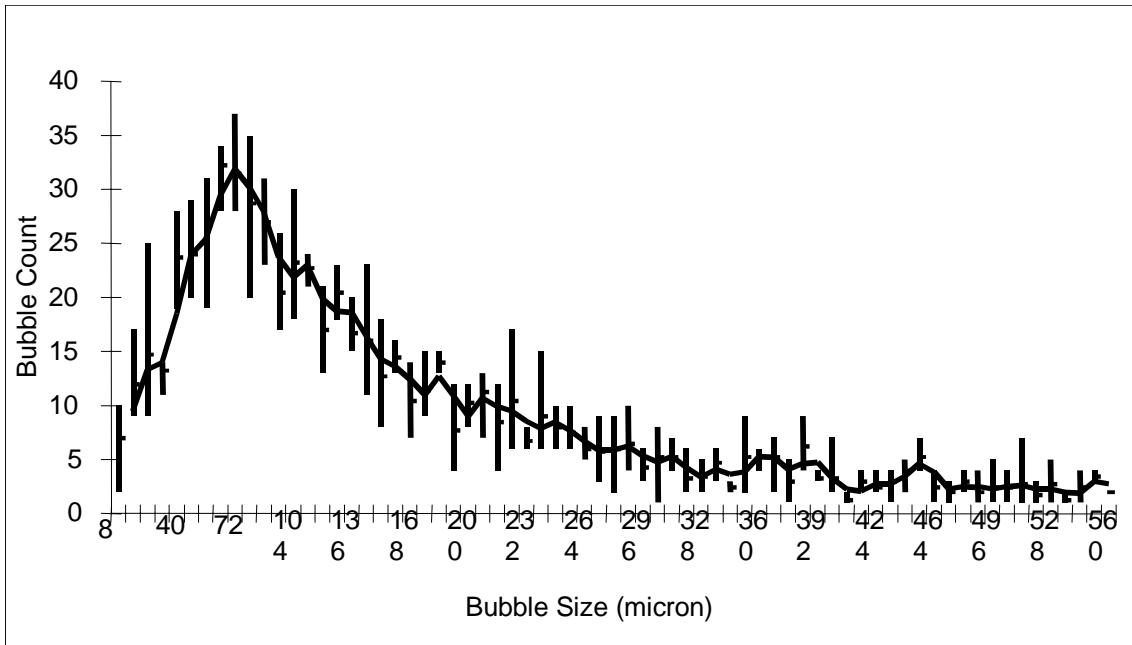


Figure 40. Repeatability test (1)

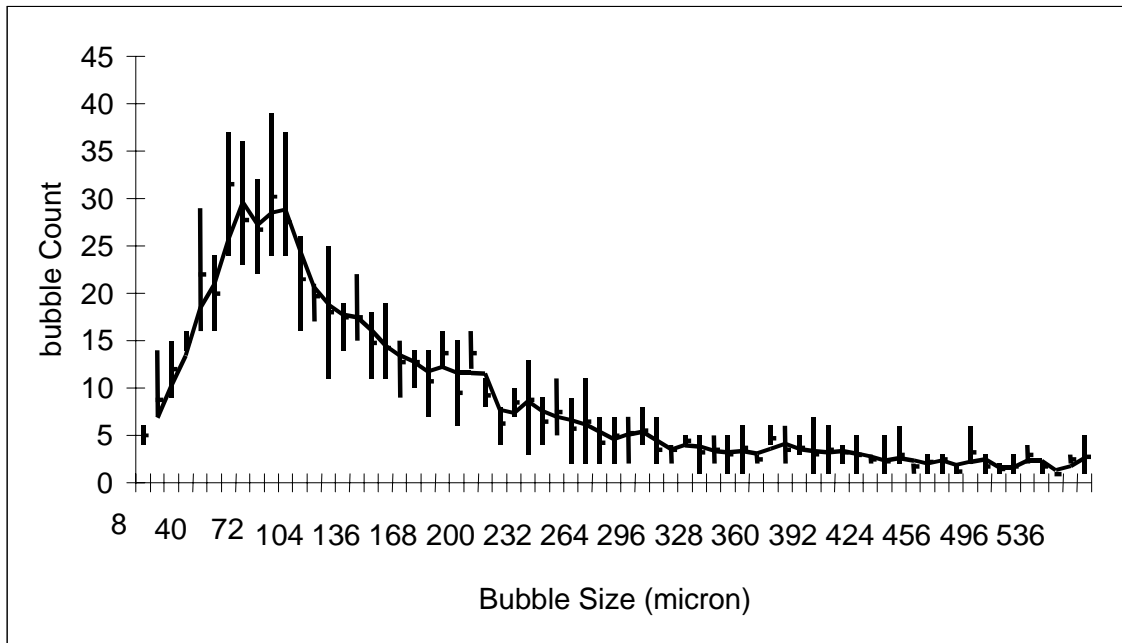


Figure 41. Repeatability test (2)

## APPENDIX-B: PENDANT DROP FOR SURFACE TENSION MEASUREMENT OF SOLUTION

Present laboratory methods for making reliable fluid sample surface tension measurements include the capillary rise, maximum bubble pressure and sessile and pendant drop. The pendant drop method explained here was employed for the measurement of the surface tension by the subcontractors of this project.

Using the profile of a pendant drop to determine the surface tension or interfacial tension of liquids has been a well-known classic and one of the most versatile methods. However, this method has never become very popular until recently due to the tedious work involved, and the lack of fast commercial instruments, also, the accuracy of the method can be quite variable depending on the drop shape and the accuracy of profile determination. With the rapid development of the digital computer and digital image processing, the situation has changed dramatically in the past 10 years. With their help we are now able to extract from a drop image its entire profile and calculate the surface tension value in a very short time and with remarkable high precision by optimizing the profile to its system equation.

The theoretical background for the calculation of the surface tension value from a profile drop has been given in the literature in detail.<sup>(8,9)</sup> When a liquid pendant drop reaches hydrodynamic and mechanical equilibrium, which is govern only by gravitational force and interfacial tension, its profile  $p(x, z)$  can be described by the equations (Figure 42).

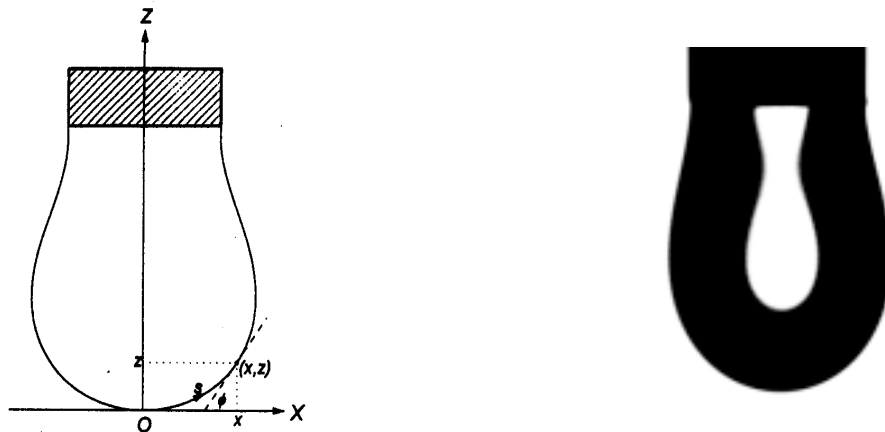


Figure 42. (Left) Geometry and notation of symbols of a pendant-drop profile  
(Right) a real pendant drop sample with air-entraining agent

$$\begin{aligned}\frac{d\phi}{dS} &= \frac{2}{B} - Z - \frac{\sin\phi}{X} \\ \frac{dX}{dS} &= \cos\phi, \quad \frac{dZ}{dS} = \sin\phi\end{aligned}\tag{2}$$

with boundary conditions at the drop apex

$$\begin{aligned}X = Z = S = \phi &= 0 \\ \frac{\sin\phi}{X} &= \frac{1}{B}\end{aligned}$$

where

$$B = \frac{1}{\alpha\kappa_{apex}}, \quad \alpha = \sqrt{\frac{\gamma}{\Delta\rho g}}.$$

Equation (2) is a special form of the general Laplace—Young equation of capillary

$$\Delta p = \gamma\left(1/R_1 + 1/R_2\right)\tag{3}$$

In the case of a pendant drop, the variable  $\alpha$  is often known in the literatures as the capillary constant, it is a constant for a given liquid-gas system.  $B$  is called the shape parameter of drops,  $\Delta p$  is the density difference between the drop and its embedding fluid phase,  $g$  is the gravitational acceleration, and  $\gamma$  is the surface tension value we are trying to determine. Apparently, the values of  $B$  and  $\alpha$  and therefore  $\gamma$  could be determined by the knowledge of the geometrical profile of the pendant drop, which can be automatically determined and optimized by the computer-aided image analysis procedure.

## REFERENCES

1. Treval C. Powers, *The Properties of Fresh Concrete*. John Wiley and Sons Inc., New York, 1968.
2. S. Mindess and J.F.Young, *Concrete*. Prentice-Hall, Inc. Englewood Cliffs, New Jersey, 1981.
3. G.M. Bruere. "Fundamental Actions of Air-entraining Agents" *International Symposium on Admixture for Mortar and Concrete*, RILEM-ABEM, 1967, pp7-23.
4. D.C.Cullum, *Introduction to Surfactant Analysis*. Blackie Academic & Professional, an imprint of Chapman & Hall, Glasgow, UK, 1994.
5. David A. Whiting and Mohamad A. Nagi, *Manual on Control of Air Content in Concrete*, Portland Cement Association, 1998.
6. G.J.Verbeck and R.A.Helmuth, Proceedings, Fifth International Symposium on the Chemistry of Cement, Tokyo, 1968, Vol. 3, pp1-32.
7. Erlin, B., "Air Content Of Hardened Concrete by a High-Pressure Method", *J. PCA Research and Development Laboratories*, 4, 1962, pp24-29.
8. Bihai Song and Jurgen Springer, "Determination of interfacial tension from the profile of a pendant drop using computer-aided image processing", *J. of Colloid and Interface Science* 184, 1996, pp64-76.
9. F.K. Hansen, "Surface tension by image analysis: Fast and automatic measurements of pedant and sessile drops and bubbles", *J. of Colloid and Interface Science* 160, 1993, pp209-217.
10. Whiting, D., Addendum to NCHRP Report 258, "Control of Air Content in Concrete, Appendix F: State-Of-Art-Report" *National Cooperative Highway Research Program Report 258*, Transportation Research Board, National Research Council, Washington, DC. March 1983.
11. Hover, K. C., "Some Recent Problems with Air-Entrained Concrete" *Cement, Concrete, and Aggregates*, CCAGDP, Vol.11, No.1, 1989, pp67-72.
12. Gay, F.T., "A Factor Which may Affect Difference in the Determined Air Content of Plastic and Hardened Air-Entrained Concrete," *Proceedings of the Fourth international Conference on Cement Microscopy*, Las Vegas, March 28-April 1, 1982, pp296-292.
13. Burg, G.R.U., "Slump Loss, Air Loss, and Field Performance of Concrete." *ACL Journal, Proceedings*. Vol.80, No.4, 1983, pp332-339.
14. Mielenz, R.C., Wolkodoff, V.E., Backstrom, J.E., and Flack, H.L., " origin, Evolution, and Effects of the Air Void System in Concrete, Part I — Entrained Air in Unhardened Concrete" *Proceedings, American Concrete Institute*, Vol. 30, No. 2, 1958.
15. Pleau, R., Plante, P., Gagne, R., and Pigeon, M. "Practical Consideration Pertaining to the Microscopical Determination of Air Void Characteristics of Hardened Concrete (ASTM C 457 Standard)" *Cement, Concrete, and Aggregates*, CCAGDP, Vol. 12, No. 2, Summer 1990, pp. 3-11.
16. S. Chatterji and H. Gudmundsson, " Characterization of Entrained Air Bubble System in Concretes by means of Image analysis Microscope," *Cement and Concrete Research*, Vol. 7, pp. 423-428, 1977.

17. J. Elsen, N. Lens, T. Aarre, D. Quenard, V. Smolej, "Determination of the W/C Ratio of Hardened Cement Paste and Concrete Samples on Thin Sections Using Automated Image Analysis Techniques" *Cement and Concrete Research*, Vol. 25, No. 4, 1995, pp827-834.
18. K.L. Scrivener and E.M. Garter, "Microstructural gradient in Cement Paste around Aggregate Particles" *Bonding in Cementitious Composites, Materials Research Society Symp. Proc.* Vol. 114, 1989, pp.77-85.
19. S.A. Roger, G. W. Groves, N.J. Clayden, and C.M. Dobson, "A Study of Tricalcium Silicate Hydration From Very Early to Very Late Stages" *Microstructural Development During Hydration of Cement, Mat. Res. Soc. Symp. Proc.* Vol. 85, 1987, pp13-20.
20. D.A.Lange, H.M.Jennings and S.P.Shah, "Image Analysis Techniques for Characterization of Pore Structure of Cement-Based materials" *Cement and Concrete Research*, Vol. 24, No. 5, 1994, pp. 841-853.
21. Harley Price Tripp, The Maximum Bubble Pressure Method for the Measurement of Surface Tension, PH.D dissertation, University of Chicago, 1934.
22. K.M. Nemati, P.J.M.Monteiro and K. L. Scrivenner, "Analysis of Compressive Stress-Induced Cracks in Concrete" *ACI Materials Journal*, Vol. 95, No. 5, 1998.
23. E.H. Lucassen-Reynders, *Anionic Surfactants: Physical Chemistry of Surfactant Action*. Marcel Dekker, INC., New York, 1981.
24. Drew Myers, *Surfactant Science and Technology*, 2<sup>nd</sup> ed., VCH Publishers Inc., New York, 1992.
25. R. Jain, R. Kasturi and Brain G. Schunck, *Machine Vision*, McGraw-Hill, Inc., 1995.
26. J. F. Young, S. Mindess, R.J. Gray and A. Bentur, *The Science and Technology of Civil Engineering Materials*, Prentice Hall, New Jersey, 1998.
27. Averill M. Law and W. David Kelton, *Simulation Modeling and Analysis*, 3<sup>rd</sup>, McGraw-Hill, Inc., 2000.
28. National Research Council, *Mathematical Research in Materials Science: Opportunities and Perspectives*, National Academy Press, Washing, D.C. 1993.
29. National Interments Co., *BridgeVIEW and LabVIEW: IMAQ Vision for G Reference Manual*, 1997.
30. Annual Books of ASTM Standards, 04.02 Concrete and Aggregates, 1992.
31. Keithley Metrabyte Co, SVC1000 Technical Reference and Software.
32. Bryant Mather, Tests of High Range Water Reducing Admixtures, Superplasticizers in Concrete, SP-62, American Concrete Institute, 1979, PP. 157-166.